2011

ELECTROSPINNING OF POLY (ESTER AMIDE)S FOR VASCULAR TISSUE ENGINEERING

Deepta Srinath

ELECTROSPINNING OF POLY (ESTER AMIDE)S FOR VASCULAR TISSUE ENGINEERING

(Spine Title: Electrospinning of Poly(ester amide)s)

(Thesis format: Monograph)

By

Deepta Srinath

Graduate Program in Engineering Science
Department of Chemical and Biochemical Engineering

Submitted in partial fulfillment
of the requirements for the degree of
Master of Engineering Science

School of Graduate and Postdoctoral Studies
The University of Western Ontario
London, Ontario

THE UNIVERSITY OF WESTERN ONTARIO
SCHOOL OF GRADUATE AND POSTDOCTORAL STUDIES

CERTIFICATE OF EXAMINATION

Supervisor	Examiners
Dr. Kibret Mequanint	Dr. Lars Rehmann
Supervisor	Dr. Jin Zhang
Dr. Amin Rizkalla	Dr. Jun Yang

The thesis by

Deepta Srinath

entitled:

Electrospinning of Poly (ester amide)s for Vascular Tissue Engineering

is accepted in partial fulfilment of the
requirements for the degree of

Master of Engineering Science

Date_____

_____
Chair of the Thesis Examination Board

Abstract

A recent surge of research in the field of tissue engineering has contributed to the development of novel biomaterials for restoring or replacing diseased cardiovascular tissues. In an effort to control biodegradability, a new class of polymers known as poly (ester amide)s (PEAs) are being studied as they show promising results for their use as biomaterials.

The work in this thesis focuses on a PEA that was synthesized from the α-amino acid L-alanine, 1,8-octanediol and sebacoyl chloride. Following detailed characterization, the synthesized PEA was used for fabricating of fibrous scaffolds with a blend of PCL by electrospinning. A number of parameters were studied in order to optimize the electrospinning process as well as fibre size; namely that of solution concentration and distance from collector. With increasing solution concentration, an increase in fibre diameter as well as pore size was observed. Conversely, increasing distance from the needle tip to the collector reduced fibre diameter for up to 10 cm then diameter increased up to 14cm from collector. In addition, qualitative and quantitative degradation of PEA and PEA-PCL polymer blend discs were also assessed and, results show that degradation proceeded primarily through fibre fusing and surface erosion. PEA quantity had a significant effect on degradation time where higher PEA contents accelerated the degradation. Finally, cell studies using human coronary artery smooth muscle cells (HCASMC) were conducted to assess its suitability for proliferation and gene expression and, consequently, use in vascular tissue engineering. MTT assay showed that the fibres were not cytotoxic. Furthermore, cells showed strong attachment after a 4 and 7 day culture. Finally, Western blot analysis revealed that elastin protein gene expression was enhanced on these fibres.

Keywords: Biomaterials, Poly (ester amide)s, electrospinning, vascular smooth muscle cells, elastin

Acknowledgements

I would like to express my sincere gratitude to my supervisors, Dr. Kibret Mequanint and Dr. Amin Rizkalla, for their guidance and advice during my study at The University of Western Ontario. I would also like to thank my lab group for their encouragement and help, in particular Darryl Knight for assisting me with polymer synthesis and Dr. Shigang Lin for his help with the cell cultures. I wish to acknowledge the Natural Sciences and Engineering Research Council of Canada (NSERC) and Western Graduate Research Scholarships (WGRS) for providing me with financial support to conduct my research. Last but not certainly not the least, I wish to thank my family for their ongoing support and encouragement.

Table of Contents

List of Figures

List of Abbreviations

AOSe	L-alanine, 1, 8-octanediol and sebacoyl dichloride Polymer
BMC	Bone marrow mesenchymal cells
CVD	Cardiovascular disease
DMF	N,N-dimethylformamide
DMSO	Dimethyl sulphoxide
DSC	Differential scanning calorimetry
ECM	Extracellular matrix
EPC	Endothelial progenitor cells
FTIR	Fourier transform infrared spectroscopy
GPC	Gel Permeation Chromatography
HCASMC	Human coronary artery smooth muscle cells
^{1}H-NMR	Proton Nuclear Magnetic Resonance
PBS	Phosphate buffered saline
PBSe	L-Phenylalanine, 1,4-butanediol and sebacoyl dichloride polymer
PCL	Polycaprolactone
PEA	Poly (ester amide)
SEM	Scanning electron microscopy
TGA	Thermal gravimetric analysis
XRD	X-ray diffraction

CHAPTER 1

1 Introduction

Cardiovascular diseases (CVDs), defined as essentially all the health conditions that affect the heart muscle, heart valves, and blood vessels, account for nearly 40% of total deaths in North America every year.[1] These typically include coronary heart disease and myocardial infarctions, with atherosclerosis serving as the primary cause.[2] Hardening of the artery wall due to the buildup of fatty materials leads to coronary occlusion and strokes, whereas loss of vessel elasticity causes aneurysms. It is estimated that an average of a million Americans succumb to heart failure every year; these diseases account for 34% of all mortality.[1] Around 500,000 Americans and 23,000 Canadians undergo coronary heart bypass surgeries every year. [1, 3] In addition, similar numbers of patients are diagnosed with heart disease every year. In order to battle this rapidly progressing condition, science and medicine have pushed the limits of biological systems to create new surgical procedures and replacement therapies.

1.1 Intervention Approaches in Cardiovascular Medicine

A preventative approach to the treatment of cardiovascular disease is advised by most health practitioners, which include strict regulations to diet and lifestyle choices. Although this may reduce the risk of the disease significantly, patients often find themselves requiring at least one form of therapy. A myocardial infarction, or heart attack, occurs at the onset of occlusion of one or more blood vessels that directly supplies to the heart.[4] If the blood flow is not restored immediately, cell death occurs within the oxygen-deprived heart muscle. Mature contracting and terminally differentiated cardiac cells, otherwise known as cardiomyocytes, cannot divide and therefore the heart tissue is beyond repair. The final result of the infarction is the formation of

scar tissue around the heart; an occurrence that is highly undesirable as scar tissue does not have the contractile, mechanical or electrical functions of a healthy myocardium.[4]

Current treatment of severe occlusion involves bypass grafts. These are usually of three different kinds: autografts, which are from the patient's own body; allografts, which are obtained from a matching healthy patient; xenografts, which are from a different species, mostly bovine or porcine tissues and finally, synthetic prostheses.[5] It can often be argued that percutaneous intervention therapies such as balloon angioplasty remain a minimally invasive procedure in an attempt to avert surgery as a treatment. However, often in more advanced progressions of the disease, this option is not generally recommended by clinicians.[6] The utilization of stents and drug eluting stents are also commonly adopted methods of therapy.[6]

In terms of other methods that are currently under extensive investigation, stem cell and gene therapies to induce angiogenesis of arteries using endothelial growth factors and the development of novel synthetic biomaterials that are used as scaffolding for differentiated cardiovascular cells or stem cells are the most promising.[6]

1.1.1 The Regenerative Approach

A major drawback of relying on surgical intervention alone is the lack of autograft and allograft donors and complications associated with post-operative immunosuppressive treatments. As a result, researchers and surgeons are continuously working on finding new methods to revive a damaged tissue. For example, the use of embryonic stem cells that can be differentiated into cardiomyocytes made cellular therapy a potential treatment for cardiovascular diseases, such as myocardial ischemia or infarctions. Recently, research has ventured into utilizing adult stem cells from bone marrow and adipose tissues. The typical mode of

administration of cell therapy is direct injection into the ventricular wall or into the coronary vessels and, is known as cardiomyoplasty.[6] Cellular therapy is a common paradigm used in tissue engineering and regenerative medicine and is often combined with tissue replacement approaches. It is advantageous in the sense that it is a minimally invasive surgery if the cells can be injected intravenously.[7, 8] Adipose tissue derived stem cells and bone-marrow derived mesenchymal stem cells are extensively studied. In the case of the former, easily accessible fat and its abundance throughout the body makes it a useful source of stem cells. [9] In one study, it was found that adipose lineage cells could function as progenitors for endothelial cells by forming a vascular-like structure in a Matrigel plug and promote neovascularization.[9] Another study demonstrated the potential of bone marrow cells forming myocardial tissue in infarcted hearts and to restore their function.[10]

Cellular therapy could potentially be effective as it can provide a renewable source of proliferative cells and differentiated cardiomyocytes which result in the regeneration of blood vessels to support and nourish these newly formed cardiomyocytes and the surrounding ischemic myocardium. In spite of the reported efficacy of this method, controversy surrounds the use of stem cells in cardiovascular tissue regeneration; in addition, there are many unanswered questions regarding its method of administration and safety.[11]

1.1.2 The Tissue Repair Approach

Given the lack of understanding, limited success, and controversy of stem cell therapy as a valuable method of intervention, a reparative approach is often studied. Vascular occlusions are often repaired by a minimally invasive balloon angioplasty. [12] In this method, a balloon attached to a catheter is guided to the site of the blockage and inflated to push the plaque against the vascular wall. This compression effect widens the narrowed vessel and increases the perfusion,

thus preventing further damage to the tissue.[12] Although the procedure is in principle a successful first-line therapy, it is not without problems. It has a tendency to lead to subsequent recoil of the vascular wall due to poor wall mechanics and restenosis of the lumen due to unregulated cell proliferation. In order to overcome these limitations, drug eluting stents are frequently deployed during the intervention. However, there are still several issues associated with this therapy, mostly that of delayed healing due to endothelial dysfunction.[13] Another concern is late stage restenosis and thrombosis. For example, in one study, if anti-platelet therapy was stopped, which occurred for some patients, occlusion was observed, which was then reversed by another percutaneous intervention, which is also prone to restenosis.[13]

1.1.3 The Replacement Approach and Tissue Engineering

When both the regenerative and the repair approaches fail to deliver the intended outcome, surgical replacement or bypass surgery of blood vessel segments is the most common intervention for coronary and peripheral atherosclerotic diseases. With the rapid growth of the elderly segment of the population, the number of coronary artery replacement interventions is expected to increase rapidly.[14] An ideal vascular graft should have adequate mechanical strength, good blood compatibility and compliance.[15] Although autologous segments of the commonly used saphenous vein or mammary artery are preferred for coronary artery bypass grafts, they are not always available and the failure rate is high. [16] Venous and arterial allograft and xenograft vessels frequently suffer from rejection; poor patency and compliance mismatch.[17] Synthetic grafts made from expanded polytetrafluoroethylene (ePTFE, Teflon) and polyethylene terephthalate (PET, Dacron) work well for large diameter vascular grafts (>6 mm ID) where the blood flow rate is high, but results in small diameter coronary artery graft applications (<4 mm ID) have been disappointing.[18] Obviously, functional restoration of diseased vascular tissues

remains a challenge and none of the existing surgical interventions provide a satisfactory outcome. Tissue Engineering has the potential to develop novel approaches to fabricate orderly and mechanically competent autologous vessels via scaffold guided in vitro engineering alternatives. Tissue engineering is an interdisciplinary field that applies the principles of engineering and life sciences toward the development of biological substitutes that restore maintain or improve tissue function or a whole organ.[15] It encompasses regenerative procedures and development of tissue for therapeutic benefits.[19, 20]

In the most frequent paradigm, tissue engineering consists of a scaffold that is porous and fabricated from a biomaterial that can be natural or synthetic and aids in the adhesion, proliferation and migration of cells. It is advantageous in the sense that it can be coupled with cellular therapy, where mesenchymal stem cells, bone marrow cells, endothelial progenitor cells or adipose stem cells can be seeded onto the scaffold to promote differentiation and proliferation, but would still require surgical placement into the patient. Biomaterials would then typically need to be compatible with the specific cells and match the mechanical properties of the tissue in question, be it myocardium patches, blood vessels or heart valves. These materials are discussed at length in a later section of this chapter.

1.2 Paradigms of Tissue Engineering

Since the development of tissue engineering, several commonly adopted strategies have been developed. These are cell transplantation, scaffold implantation, a combination of the two or, *in vitro* tissue engineering.

As mentioned in the preceding section, cell transplantation typically involves the injection of cells into the area of a damaged tissue.[4, 6] In myocardial tissue engineering, it is

possible to isolate mesenchymal stem cells from adult bone marrow and inject it into the affected myocardium. A typically minimally invasive procedure, cell transplantation is an appealing option. However, there is absolutely no guarantee that the injection of cells into the area will form a functional network of cells. [2] The biggest concern in cellular therapy is immune rejection which could eventually lead to loss of specified cellular function.[19, 21] Efforts to improve immune rejection are currently being looked into, possibly with simultaneous administration of immunosuppressant along with the cell injections.[9, 10] Another potential issue in the future is commercial availability. If clinical trials are successful, it may be difficult to meet commercial demand for clinical need of cardiovascular treatments.[4]

A very common strategy of tissue engineering involves the implantation of a scaffold into the host model that helps repopulate and regenerate damaged tissue.[22] Regeneration is achieved by implantation of a resorbable matrix that remodels *in vivo* and thus produce a fully functional heart valve complete with connective tissue proteins.[23] Repopulation is yet another approach, where a decellularized connective tissue is prepared for human cell proliferation thereby reviving the cellular matrix from within the patient and creating an entirely functional tissue.[23] Sadly, the studies resulted in several failures and early patient deaths and efforts are being made to invest more time and money into scaffold implantation research.[22] A major contributor to the failure of this method is poor cell recruitment and maintenance, as it is entirely dependent on the native cells to populate the valve.[23]

Another form of implantation is cell-seeded scaffolds, where a matrix substrate is seeded with cells prior to implantation into the host, without primary *in vitro* maturation.[22, 24] It typically consists of a substrate on which growth factors are combined; so upon implantation, cells from the body are further recruited to the site of scaffold to mature and form tissue. [22] The

incorporation of vascular endothelial growth factor (VEGF) to provide controlled release into a polymeric substrate has been reported. Release of bioactive VEGF was confirmed using the specified assays and demonstrated that the growth factor retained its angiogenic properties and encouraged neovascularization around the scaffold.[22] A key issue in these studies is generally matching growth factor release to the kinetics of physiological responses. [22]

Lastly, *in vitro* tissue engineering is the most commonly utilized paradigm. It typically involved seeding cells on a scaffold that is usually a polymeric substrate, either from naturally occurring materials or synthetic and placing it in a bioreactor until complete maturation.[2] The seeded cells will infiltrate the scaffolds and proliferate while the scaffold undergoes degradation, if required. This way, cells are able to lay down their own ECM and the substrate acts as a temporary matrix until new ECM is formed. [25] Finally, the matured tissue is ready for implantation into the host, allowing further *in vivo* maturation. Points of consideration with these studies are the choice of cells, scaffolds and bioreactors that are used.[22, 25] Isolated multipotent cell varieties are usually utilized as they can differentiate into a variety of tissue specific cells and do not cause significant host responses. These cells would typically include fibroblasts and endothelial cells, where *in vitro* proliferation is quick, while using adult smooth muscle cells or cardiomyocytes provide almost no proliferation. In addition, the scaffold material is extremely important as it regulates cell adhesion and proliferation. Furthermore, if a biodegradable substrate is required so the eventual tissue is completely comprised of native ECM, the supporting material should be tailored accordingly.[26, 27] Finding the right material thus remains one of the key challenges faced when pursuing *in vitro* tissue engineering.

1.2.1 Clinical Need for Vascular Tissue Engineering

As mentioned earlier, the prevalence of cardiovascular disease in North America is high and subsequently contributes to high mortality rates.[1] It is a tremendous economic burden and therefore, new medical advances are emerging to tackle this burden. With the development of percutaneous interventions such as balloon angioplasty and stent placements, the burden was thought to have been considerably lowered; however, it remains that bypass surgery to repair coronary artery disease is probably the most routine method adopted by clinicians.[14] Vascular grafts are usually comprised of saphenous vein, which has shown to lead to aneurysms in some patients due loss of elasticity when exposed to arterial pressure.[28] As stated above, synthetic vascular grafts are used despite their poor performances.[28] Thus, the need to improve current therapeutic approaches is high. Surgeons, clinical researchers and biomedical engineers are always exploring new methods, which is where tissue engineering for vascular replacement shows immense promise. Providing cells with a substrate that mimics the physiological matrix and having the ability to repair, grow and remodel create the premise for an efficient approach to complete tissue fabrication and functionality. Although cardiovascular tissue engineering is far from success, studies are showing promising results as to its viability in future vascular intervention.[24, 29, 30] For example, development of an autologous tissue-engineered graft for hemodialysis patients in a multicentre clinical trial showed maintenance of patency upto six months after implantation.[31] The potential benefit of engineered vascular tissues is significant. Currently patients who had vascular surgery must take life-long anticoagulant drugs to mitigate graft rejection.[24] Patient-specific tissue-engineered blood vessels will eliminate the need of drugs since the tissue will not be rejected. The potential impact of the proposed research is even more significant for pediatric patients since tissue-engineered vessels have the capacity to grow, repair, and remodel as required with normal development.

1.2.2 Three Dimensional Tissue Model

In addition to having a clinical application, engineered vascular tissues could have diagnostic applications for testing drug uptake and metabolism, toxicity, and pathogenicity contributing to our understanding of genetic or environmental factors regulating treatment outcomes. The use of cell and organ culture in combination with animal models to study vascular diseases (e.g. atherosclerosis, post angioplasty restenosis, and hypertension) in an attempt to develop therapeutics is not new but employing engineered human vascular tissues for this role is a novel concept.[32, 33] While conventional 2D cell cultures are indispensable to our understanding of tissue morphogenesis and function in physiological and pathological states, they do not accurately replicate the 3D microenvironment of human tissues. For example, 2D culturing of vascular cells for studying intimal hyperplasia without the arterial wall structure and extracellular matrix cannot recapitulate the intricate vascular wall mechanics and morphogenesis.[32, 34] Similarly, animal organ cultures and whole animal models do not completely mimic the human biology due to the inevitable inter-species difference. Studies using closely related nonhuman primates are constrained by limited availability, legal restrictions, ethical concerns, and high cost.[32]

When studying human vascular diseases and therapeutics, a realistic model is a human tissue but, the inability to experiment directly on human subjects limits this progress. Thus the need for an engineered human vascular tissue model to close this gap is of vital importance. Engineered vascular tissues are not likely to replace animal or human subjects; however, they have the potential to provide high throughput, substantive, and detailed information regarding very specific conditions under controlled environments. The significance is far-reaching as these "made to order" vascular tissues comprising cells (smooth muscle and endothelial cells) and

ECM (elastin and collagen) could serve as a powerful high-throughput tool to study disease models and therapeutic outcomes that are not possible with animal-based models.[35, 36] In this context, engineered vascular tissue technology may be used both to validate drug targets and to optimize loads. This allows for cardiovascular drug screening in a more controlled and efficient way than can be performed using a traditional whole animal approach, thereby minimizing the number of laboratory animals used and decreasing the overall cost of performing research.[35] The use of 3D engineered tissue to reduce the cost and time required for physiological genomic research is another niche which is unexplored. Recently engineered 3D tissues such as cardiac patch [37], lung tissue [38], cornea [39] and solid tumor models [40] have emerged as powerful tools for drug discovery and to study cells in 3D.[41] In comparison with 2D cultures, 3D cell models create a more realistic representation of real tissues, which is critical for many important cell functions, including morphogenesis, cell metabolism, gene expression, differentiation, and cell-cell interactions. [41]

1.3 Requirements of Tissue Engineering Scaffolds

Tissue engineered scaffolds act as a support mechanism during tissue repair, regeneration or fabrication process, or serve as a complete replacement to the damaged tissue. Scaffolds can either be fabricated from naturally occurring polymers such as elastin [42], collagen [43], silk [44] or more commonly, from synthetic polymeric biomaterials.[8] Different configurations of scaffolds can be constructed and it is often dependent on the type of engineering application it is required. In order for a tissue to be constructed, the biomaterial of choice needs to fulfill certain characteristics that allow for maximum performance. These criteria are essentially used as a checklist when developing a new scaffold and are extremely important.

Fabrication methods ensure a diverse range of configurations; it also helps control parameters such morphology and mechanical properties.[20] For example, electrospinning is able to provide a fibrous mesh where pore size and fibre size can be tailored to be on the nano-scale.[45] In addition to modification of scaffold architecture based on its application, porosity of the scaffold also needs to be considered. This includes pore size measurements as well as the distribution of the average pore size across the construct, to promote cell infiltration and organization.[45-47] Optimization of surface chemistry will also allow better cell adhesion, proliferation and migration.[45, 48]

Given that these scaffolds are being designed for use in medicine, the materials used obviously need to be biocompatible. Biodegradability is also another desired characteristic, wherein degradation and tissue regeneration occur at a constant and predictable relationship.[38] Mechanical properties such as tensile strength and elastic modulus are important when considering a new biomaterial as well, as the substrate should provide support to the cells until local extracellular matrix is synthesized.[49]

1.3.1 Naturally Occurring Polymers

Natural ECM components such as collagen and fibrin are commonly used polymers for tissue engineering. [45, 50] Modified polysaccharides such as chitosan and cellulose are also actively studied. [51] It can be inferred that given these are naturally occurring, the probability of an immune host response is negligible. They provide a natural substrate for cell migration and adhesion and therefore, are among the favorite group of polymers studied. Decellularized tissues have been utilized as well, although it has shown poor repopulation *in vivo*.[45, 52] There has been some evidence on immunogenic responses by the body to foreign collagen. [53] For such cases, the process of cross linking has been suggested with satisfactory results.[54] Mechanical properties and

degradation rates are however, proven to be extremely difficult to control in naturally occurring polymer scaffolds.[54]

1.3.2. Synthetic Polymers

Synthetic polymers are essential materials in tissue engineering due to their varied but controllable processing characteristics. Another added advantage is the ability to design and modify their chemical structure as per requirement, which can consequently be used to tailor degradation rates, if needed, and mechanical properties as well.[55]

Since the advent of tissue engineering as an approach in biomedicine, polyester based materials have reigned as the materials of choice. These include poly (lactic acid) (PLA)[56], poly (glycolic acid) (PGA)[56], their copolymers, poly (urethane), [44] poly ε-caprolactone [57] and poly (hydroxybutyrate) (PHB). [58] In longer culture periods, PLA degradation releases lactic acid by-products which significantly altered the pH of the region, which in turn led to tissue inflammation and some necrosis. [59] This can be translated to all acid based polymers such as butyric acid and glycolic acid as well. Both PGA and PLA have been used in several clinical applications. For example, PGA has been used as a suture [60], scaffolds for cardiac tissue engineering [4], vascular tissue engineering [61], and valvular tissue engineering [62]. Similarly, PLA has also been used in 3D tissue models and has shown slightly higher resistance to hydrolytic degradation due to increased hydrophobicity.[63]

Other materials studied for vascular tissue engineering are polyurethanes. Polyurethanes are synthesized from diols and di-isocyanates, the latter of which may potentially release toxic degradation by-products.[64] This class of synthetic materials is in wide industry use as well as in biomedical engineering. Polyurethanes are easily compliant and show good mechanical

characteristics and biodegradability. [60] Not only is it possible to create a polyurethane structure that lasts a long time *in vivo* to function as a permanent prosthesis, but degradation time can be varied to produce a scaffold that only lasts a few days.[60] It has been shown that medical grade polyurethane scaffolds are also effective in maintenance of differentiated smooth muscle cell phenotype.[65]

1.3.3 Biodegradable Polymers

As mentioned earlier, PLA, PGA and their copolymers have been of great interest in the biomedical field for quite some time; this is largely attributed to their biodegradable nature. In tissue engineering, biomedical devices such as sutures, scaffolds, drug delivery vehicles and surgical implants are often developed to be biodegradable and to elicit minimal foreign body response.[60, 66] Of these, aliphatic polyesters such as PLA and PGA have been the most widely investigated in the past years. Despite their degradable nature, polyesters do not possess tunable degradation characteristics. This is largely in part due to their synthesis from one monomer alone. [57] In order to make them tunable for biodegradation, copolymerization of polymers or blending is adopted which is not successful all times.[60] Another concerning issue, as previously mentioned, is the toxicity of the acidic degradation products of these polyesters; this is not suitable in a cellular environment and therefore limiting the use for *in vivo* tissue engineering.

Recent renewed interest however, has been directed at addressing these issues and concerns faced by aliphatic polyesters. A group of novel poly(ester amide)s (PEAs) comprised of α-amino acids have been suggested for use in biomedical applications; this family of polymers has tunable characteristics and are compliant both for hydrolytic and enzymatic degradation.[67, 68] Their degradation products are not likely to be toxic due to their physiological origin; they have also shown to be to prone to cleavage by enzymes such as chymotrypsin.[67] Puiggali et al used

interfacial condensation to develop crystalline PEAs using amino acids glycine, L-alanine and L-D,alanine.[67, 69-71] A preliminary biodegradation study showed that these PEAs degrade both hydrolytically and enzymatically and that degradation rate varied with stereospecificity.[71, 72]

Katsarava and his coworkers reported a family of PEAs derived from solution polycondensation of di-p-toluenesulfonic acid salts of alkylene diesters and di-p-nitrophenyl esters of diacids. [73, 74] These PEAs were shown to have a range of molecular weights and were suitable for the controlled drug release and gene therapy. Recent research from the same group developed PEA microspheres with high encapsulation efficiency that were loaded with paclitaxel, a drug used both for the treatment of various types of cancer and cardiac restenosis.[75] As there is only a handful of evidence about these PEAs for use in biomedical applications as compared to other aliphatic biodegradable polyesters, this work attempts at developing a PEA for vascular tissue engineering applications, which are further outlined in section 1.5.

1.4 Scaffold Fabrication Methods

There are a number of scaffold fabrication methods used for tissue engineering; the ones outlined below are freeze drying, fibre-bonding, solvent casting/particulate leaching and finally, electrospinning.

1.4.1 Freeze Drying

In the freeze drying method, the polymer is dissolved into a suitable solvent which is then added to water to obtain an emulsion.[66] The solvent is then removed by lyophilization under high vacuum, thus leaving a porous substrate. The resulting constructs are foams, which have capillary type pore structures. It is typically used for scaffolds to be fabricated from collagen, which are usually heat sensitive.[43] However, the capillary type pores that are formed are often

irregular in size and may not be suitable for cell seeding. Recent studies however aim at addressing this issue to obtain more uniform pore sizes by altering techniques such as freezing rates or controlling temperatures.[43]

1.4.2 Fibre Bonding

In this method first developed in 1994, polyglycolic acid (PGA) fibres are immersed in a poly (lactic acid) (PLA) solution, and the solvent is evaporated allowing the PGA fibres to embed in the PLA. By heating beyond the melting temperatures of both polymers, the PLA melts first, filling the voids left by the fibres, and as the PGA begins to melt, the fibres weld together.[76] The PLA is then dissolved out from the composite in methylene chloride, leaving behind porous PGA mesh, with pore sizes ranging from 30-35 μm, the largest value being around 200μm. [76] A further modification proposed by this technique is combining it with freeze drying and emulsification. After removing PLA, distilled water was added to form an emulsion. The mold was then quenched in liquid nitrogen and freeze dried to remove water and the methylene chloride. Combining the two methods allowed for control of pore sizes and overall porosity.[76]

1.4.3 Solvent Casting/ Particulate Leaching

For this method, both degradable and non-degradable polymers that are soluble in an organic solvent of choice are employed. [64] The actual process makes use of the chosen polymer in a solution; often chloroform or methylene chloride is used. Sieved porogens such as ammonium chloride, sodium chloride or paraffin particles are then added to this solution and the solution is air dried or evaporated in vacuum overnight to obtain a polymer and salt mixture. Subsequent washing of this mixture with a second solvent, such as water or in the case of paraffins, hexane, then leach the porogen out, leaving a highly porous polymer. [4] In order for this

method to work effectively, the solvent dissolving the polymer must not dissolve the porogen and the second solvent dissolving the porogen must not affect the polymer.[77]

The pore size, interconnectivity and porosity of the scaffold is controlled by the amount and size of the porogen that is added to the solution.[77, 78] This property and the fact that the method is relatively simple allow solvent casting and particulate leaching suitable for scaffold fabrication. The technique does, however, pose some disadvantages. When the porogen is dissolved into the polymer solution, the prevailing difference in densities of the salt and polymer leads to a non uniform distribution.[78] Consequently, when the polymer-porogen mixture is washed out after evaporation of the solvent, the uneven distribution does not allow for complete leaching of the porogen. The final scaffold therefore usually has a small concentration of porogen enveloped in its pores. Additionally, during solvent evaporation, the formation of a solid layer causes the organic solvent to be trapped in the final structure. Also, the amount of time required to completely wash the porogen out and produce the scaffold is tedious and slightly cumbersome.[78] This method generally produces irregular pores with sizes between 30-300 μm.[4]

1.4.4 Electrospinning

This method is another widely used approach to produce scaffolds and is effective in producing tubular constructs in fibrous configurations, which are useful when mimicking the extracellular matrix. Electrospinning has been known since 1902, when Cooley and Morton produced fibres using this process.[21, 79] However, it was not until the mid 1990s that research in electrospinning was applied to fabricate tissue engineering scaffolds. The significance of electrospinning is mainly due to the potential of this method to create fibres of diameters ranging from submicron to nanometers. A typical laboratory setup consists of a high voltage source, a grounded collector and a syringe pump. The polymer is dissolved in a solvent; this solution is

then forced through a needle using a syringe pump. This needle is connected to the high voltage supply, which induces charge into the solution. When the electric potential of the surface exceeds a certain critical value, the surface tension is overcome and the solution erupts from the end of the needle, forming a Taylor cone.[79, 80] As the jet of solution erupts, it undergoes a whipping instability, which increases the travel time as well as the total path length of the fibre to the grounded collector; the increased time allows for maximum solvent evaporation and the path length creates thinning of the fibre. [45, 81, 82] Several configurations can be employed for the collector, such as a stationary plate or a rotating mandrel. [21, 79] Utilizing a stationary collector creates a randomly oriented fibre mat, whereas a rotating mandrel provides more control and produces an aligned fibre mat. [79-81]

The versatility of scaffolds that can be produced using electrospinning serves as a significant advantage when developing vascular tissue constructs. It also allows for enhancement of mechanical properties such as tensile strength by manipulation of process parameters (mandrel speed, distance from collector, etc). As mentioned previously, the geometry of the scaffold can be influenced by the collector configuration; a rotating mandrel is used so that a tubular structure for coronary arteries can be formed, if mats are required then the grounded collector is a flat surface.[79, 83] The disadvantage associated with this method is that smaller inter-fibre spacing causes some issues with cell infiltration during cell delivery and fostering. Despite this, electrospun nanofibres best mimics several ECM proteins.[19, 83]

1.5 Objectives and Rationale

There are several biomaterials that are currently being studied as scaffolds in tissue engineering and regenerative medicine. Among these poly (ester amide)s are one of the emerging candidates since they can be tunable in terms of their degradation rate and, also the degradation

products may not be toxic. These properties can reduce the limitations prevalent in other synthetic polymers that are currently used. This work focuses on developing a novel PEA for use as scaffolds for vascular tissue engineering. To fabricate scaffolds, electrospinning is proposed to produce fibrous constructs that could potentially mimic the structure of the natural ECM. In addition, fibres produced by electrospinning can be controlled to very small diameters, typically smaller than that of a cell, thereby prompting cell adhesion, proliferation and migration.

In view of the above, the objectives of this study were to:

- Synthesize and characterize a poly (ester amide) from L-alanine, 1,8-octanediol and sebacoyl chloride;
- Fabricate scaffolds by electrospinning and optimize electrospinning parameters;
- Conduct biodegradation studies under physiological conditions;
- Assess the interaction of human coronary artery smooth muscle cells (HCASMCs) with these electrospun scaffolds.

CHAPTER 2

2 Materials and Methods

2.1 Materials

ε-Polycaprolactone of molecular 80,000 Da was purchased from Solvay Products (Capa® PCL, Perstorp Group, Sweden) and *p*-toluenesulfonic acid salt was purchased from JT Baker (Phillipsburg, NJ). All solvents were procured from Caledon Labs (Georgetown, ON). All other chemicals, including L-alanine were obtained from Sigma Aldrich (Milwaukee, WI) and were used as received.

2.2 Methods

2.2.1 Monomer Synthesis

L-alanine (5.0 g, 56 mmol, equivalent to 2.2 mol), *p*-toluenesulfonic acid• H_2O (11.67 g, 61 mmol, equivalent to 2.4 mol) in 125 mL of toluene was suspended in a three-necked round bottom flask with a stirrer and refluxed at 140°C while attached to a Dean-stark apparatus for 2 hours to remove all traces of residual water. 1, 8-octanediol (3.7 g, 26 mmol, equivalent to 1.0 mol) was subsequently added and heated in an oil bath and refluxed for a period of 40 hours. The resulting mixture was cooled to room temperature, filtered and then recrystallized twice from 30 mL of isopropanol to provide the monomer.

^{1}H-NMR (400 MHz, DMSO-d_6) : δ 8.26 (br s, 6H, -NH_3^+ TsO^-), 7.48 (d, 4H, J=8.2, Ar-*H meta* to CH_3), 7.12 (d, 4H, J=7.8, Ar-*H ortho* to CH_3), 4.2-4.08 (m, 6H, -C(O)O-CH_2-, -C_αH), 2.29 (s, 6H, Ar- CH_3), 1.64-1.57 (m, 4H, -C(O)O-CH_2-CH_2-), 1.38 (d, 6H, J=7.2, -C_αH- CH_3), 1.35-1.25 (m, 8H, C(O)O-CH_2-CH_2-(CH_2)$_4$-). Yield: 85%

Another monomer was synthesized in a similar manner using L-phenylalanine and 1, 4-butanediol.

^{1}H-NMR (400 MHz, DMSO-d_6) : δ 4.25 (br s, 6H, -NH_3^+ TsO$^-$), 7.48 (d, 4H, J=8.39, Ar-*H meta* to CH_3),7.11-7.09 (d, 4H, J=7.8, Ar-*H ortho* to CH_3), 4.2-3.95 (m, 6H, -C(O)O-CH_2-, -C_αH), 2.27 (s, 6H, Ar- CH_3), 1.64 (m, 4H, -C(O)O-CH_2-CH_2-), 1.32 (d, 6H, J=7.2, -C_αH- CH_3), 1.33-1.29 (m, 8H, C(O)O-CH_2-CH_2-(CH_2)$_4$-). Yield: 85%

2.2.2 Polymer Synthesis

Interfacial polymerization was used to obtain the polymers. Sebacoyl chloride (1.20 g, 0.005 mol) in 15 mL of dichloromethane in an addition funnel was added dropwise to either of an aqueous solution of the monomers (3.16 g for AOSe and 3.64 g for PBSe, 0.005 mol) and sodium carbonate acting as the proton acceptor (1.06 g, 0.010 mol) until completion. The mixture was stirred at room temperature for 12 hours and then dichloromethane and water were extracted with a rotary evaporator at a temperature of 50°C and 100°C respectively. The resulting polymer was purified using Soxhlet extraction for 48 hours and dried under vacuum at room temperature.

^{1}H-NMR for AOSe(400 MHz, DMSO-d_6) : δ 6.18 (d, 2H, J=7.27, -N*H*-CO-) 4.59, (m, 2H, -C_αH), 4.16-4.09 (m, 4H, -C(O)O-CH_2-), 2.24-2.17 (m, 4H,-NH-C(O)-CH_2-), 1.66-1.63 (m, 8H, -C(O)O-CH_2-CH_2-, -NH-C(O)O-CH_2-CH_2-), 1.3-1.23 (m, 22H, -C_αH- CH_3, C(O)O-CH_2.CH_2.(CH_2)$_4$-, -NH-C(O)-CH_2-CH_2-(CH_2)$_4$-).

^{1}H-NMR for PBSe(400 MHz, DMSO-d_6): δ 7.7-7.2 (Ar-H), 4.25 d, 2H, J=7.27, -NH_3^+CHOO-), 4.10 (m, 4H, -C(O)O-CH_2-) 3.20 (CH_2-Ar), 2.25 (m, 2H, CH_3-Ar), 1.65 (-COOCH_2CH_2), 1.20 (-CH_2)

Figure 1 shows the reaction scheme for the polymerization to obtain the poly(ester amide).

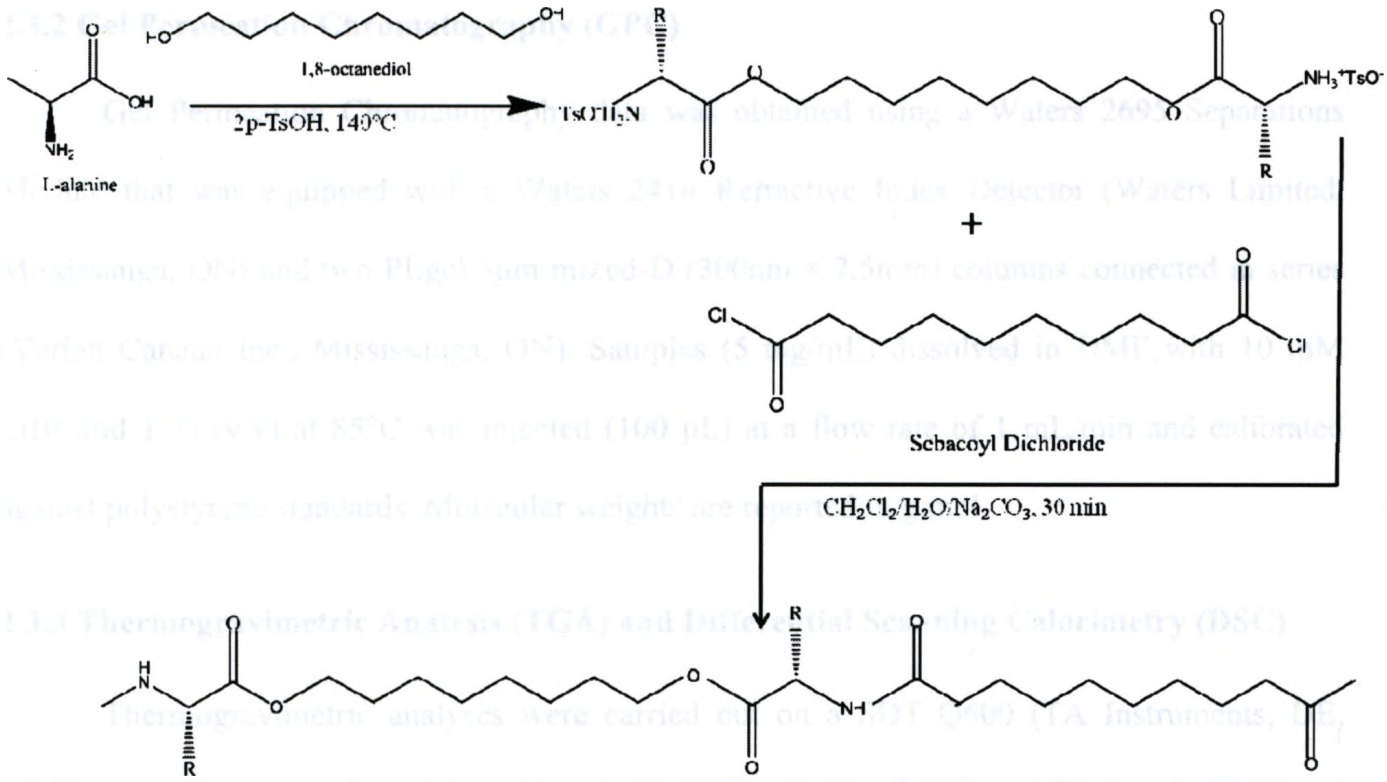

Figure 1: Synthetic scheme for PEA from L-alanine, 1, 8-octanediol, sebacoyl chloride

2.3 Polymer Characterization

2.3.1 Spectroscopic Analyses

^{1}H-NMR (400 MHz) spectra were obtained on a Varian Inova 400 spectrometer (Varian Canada Inc., Mississauga, ON). Chemical shifts are reported in parts per million (ppm) and are calibrated against residual solvent signals of dimethyl sulfoxide (DMSO, δ 2.5 ppm). All coupling constants (J) are reported in Hertz (Hz). Fourier Transform Infrared (FTIR) spectra were recorded by averaging 32 scans at a resolution of 1/cm using Bruker Vector 22 spectrophotometer.

2.3.2 Gel Permeation Chromatography (GPC)

Gel Permeation Chromatography data was obtained using a Waters 2695 Separations Module that was equipped with a Waters 2414 Refractive Index Detector (Waters Limited, Mississauga, ON) and two PLgel 5μm mixed-D (300nm × 7.5mm) columns connected in series (Varian Canada Inc., Mississauga, ON). Samples (5 mg/mL) dissolved in DMF with 10 mM LiBr and 1 % (v/v) at 85°C was injected (100 μL) at a flow rate of 1 mL/min and calibrated against polystyrene standards. Molecular weights are reported in g/mol.

2.3.3 Thermogravimetric Analysis (TGA) and Differential Scanning Calorimetry (DSC)

Thermogravimetric analyses were carried out on a SDT Q600 (TA Instruments, DE, USA) under dry nitrogen at a heating rate of 20°C/min (for AOSe and polymer blends) and 10°C/min for PCL, up to 600°C. Differential scanning calorimetry was performed on a DSC Q200 V24.2 Build 107 (Mettler-Toledo GmBH, Switzerland) at a heating rate of 10°C/min from -50 to 200°C. All samples prepared ranged from 2 to 5 mg and glass transition temperatures (T_gs) were obtained from the second heating cycle.

2.3.4 X-Ray Diffraction (XRD)

X-ray diffraction was carried out on a Rotaflex RTP 300RC (Rigaku, Japan) to assess the crystallinity of the synthesized PEA and polymer blends. It was run at 10°/min at a step size of 0.02 and between 2θ angles of 5-65° and cobalt α-radiation of 45kV and 160mA.

2.3.5 Fourier Transform-Infrared Microscopy (FT-IR)

Fourier Transform Infrared (FTIR) spectra were recorded by averaging 64 scans at a resolution of 1/cm using Vector 22 spectrophotometer (Bruker, MA, USA) to characterize peaks of both monomer and PEA.

2.4 Scaffold Fabrication

2.4.1 Electrospinning of PEA to form Fibrous 3D Mats

Varying concentrations of PEA in chloroform, ranging from 15%-30% w/w were electrospun at optimized parameter values at a voltage of 13 kV, flow rate of 0.08 mL/h and varying distances of 7, 8 and 9 cm from the collector. Varying amounts of PCL at a fixed concentration of 8% w/w in chloroform were used as viscosity modifiers and added to each sample. The PEA-PCL solutions were then continuously stirred in a sealed beaker under the fume hood for 1.5 hours in order to ensure homogenous mixing. Due to this, the final concentrations of all the samples varied from 14-21.5%, in varying compositions of PEA to PCL. These ratios are as follows (PEA:PCL): 65-35, 70-30, 75-25, 80-20 and 82-18. After Fibres were obtained, they were dried in a fume hood at room temperature for 24 hours and then slowly peeled off from the aluminum foil.

2.5 Scaffold Characterization

2.5.1 Scanning Electron Microscope (SEM)

Fibre morphology of the scaffolds for each of the electrospinning condition as well as degradation studies was visualized using SEM, (S-2600N, Hitachi, Japan). Samples were mounted on carbon-taped aluminum stubs and gold-sputtered at 15 mA for 1.5 minutes prior to analysis. In order to assess fibre diameter and pore size distribution, ImageJ software (NIH, Bethesda, MD, USA) was used to obtain a sample size of 100 Fibres or 100 pores.

2.6 Degradation Study

Both qualitative and quantitative degradation studies were carried out. Due to the fact that the PEA was not suitable for electrospinning on its own, PEA discs were used as a control. For qualitative analysis, all other samples used were obtained by electrospinning at the specific

concentrations as mentioned in the preceding section. Samples measuring 20mm by 20mm (n=3) were cut, using scissors and were placed in vials containing 10mL of phosphate buffered saline (PBS) at a pH of 7.4. All samples were incubated at 37°C for up to 28 days. Prior to SEM analysis, samples were taken out of PBS, rinsed several times with distilled water and then dried under vacuum at room temperature overnight.

For quantitative studies, discs were used so as to standardize the measurements throughout the experiments. Samples used for degradation of polymer films, (PEA and PCL) were obtained by heat pressing at 150°C and 200kPa for 2 minutes. Polymer blend films however, were obtained by dissolving the samples in chloroform at the specific concentrations and then by casting in a circular aluminum pan. The solvent was allowed to evaporate overnight and then the resulting cast was heat pressed at the same conditions as above. Polymer discs of 12 mm in diameter were then punched out and were weighed prior to incubation. They were then incubated in vials at 37°C containing 10 mL of PBS for up to 28 days. Prior to weighing, samples were taken out of PBS, rinsed with distilled water and then dried under vacuum at room temperature.

2.7 Cell Proliferation, Cytotoxicity and Western Blot Analyses

Samples were prepared for cell cultures by punching out heat-pressed PEA films into small 12 mm diameter discs, and punching out electrospun polymer blend mats of varying concentrations and electrospun PCL films at 8%w/w. All samples were affixed to coverslips using silicone grease and sterilized by immersion in ethanol for 30 minutes. The films were then washed with PBS and transferred to a 24-well cell culture plate (BD Biosciences, San Jose, CA)

and incubated in 1mL of culture medium at 37°C overnight. Following this, cell seeding was carried out as follows:

Human coronary artery smooth muscle cells (HCASMCs; Cambrex Biosciences, Walkersville, MD) between passage 6 and 10 were used to evaluate the attachment and spreading of vascular cells on PEA films, PEA-PCL electrospun mats and control PCL mats. HCASMCs were cultured in SmGM-2 (smooth muscle growth medium-2 with Bullet Kit; Cambrex) supplemented with 1% penicillin/streptomycin solution (P/S). Cultures were maintained in a humidified incubator at 37°C and 5% CO_2. HCASMCs were seeded onto films at an initial cell density of approximately 10^4 cells/cm^2 and cultured for 4 and 7 days before fixation and immunostaining. Following culture time, cells were fixed at 4°C for overnight in 4% paraformaldehyde (EMD Chemicals, Gibbstown, NJ) in divalent cation-free PBS and permeabilized with 0.5% Triton X-100 in PBS. HCASMCs were incubated for 1 hour at ambient temperature in 1% BSA/PBS containing Alexa Fluor® 568 phalloidin (Invitrogen, Eugene, OR; 1:50 dilution). Hoechst 33342 (10 μg/mL; Sigma-Aldrich) dissolved in PBS was used to label nuclei. Cover-slips were mounted on glass slides in Vectashield (Vector Laboratories, Burlington, ON) and then sealed with nail enamel. Imaging of samples was carried out on a Leica DM-IRB fluorescence microscope equipped with epifluorescence and the appropriate filters (Leica, Canada).

For cytotoxicity, 3-(4,5-dimethylthiazol-2-yl)-2,5-diphenyltetrazolium bromide (MTT) assay was carried out following the manufacturer's protocol (Vybrant®, Invitrogen, Burlington, ON, Canada). Cells were seeded onto electrospun PEA-PCL mats as well as PCL and PEA control films. The initial cell density was 6×10^4 cells/scaffold in 96-well tissue culture plates which were then cultured for 4 days. An MTT solution was added to each well to make the final

concentration 1.10 mM and then incubated at 37°C. After removal of the supernatant, dimethyl sulphoxide (DMSO) was added; absorbance was recorded at 550 nm by a plate reader and quantified using a standard curve. Negative control experiments were carried out by adding MTT to the culture medium only.

Finally, Western blot analysis was used for elastin expression and HCASMC phenotypic marker proteins. Following specified culture times, cells were washed three times at specific with ice-cold PBS and whole cell lysates were obtained by harvesting cells in 100 µl of sodium dedecylsulphate (SDS) electrophoresis sample buffer containing 5% (v/v) β-mercaptoethanol. Lysates were sonicated and then followed by microcentrifugion. Protein concentrations were determined by 660 nm Protein Assay (Thermo Scientific, Ottawa, Canada). Protein samples (80 µg for evaluating elastin expression were separated by 10% SDS-PAGE and subsequently transferred at 90 V for 1 hour at 4°C to nitrocellulose membrane in a Tris-glycine buffer. The membranes were blocked by the utilization of 5% nonfat dry milk in PBS and were incubated overnight at 4°C with primary antibodies (monoclonal mouse anti-elastin at 1:200; anti-SM-α-actin and anti-GAPDH at 1:2000; all others at 1:1000). Transfer efficiency and homogeneous loading was verified by Ponceau red stain. The blots were then labeled with Alexa 680- and IRDye 800-conjugated secondary antibody (Invitrogen, Burlington, ON, Canada), and labeled proteins were visualized by the Odyssey system (LI-COR Biosciences, Lincoln, NE). Protein bands on the Western blots were quantified using Gel-Pro Analyzer (Version 4.0) software and the results were normalized as the ratio of elastin, SM-α-actin, and calponin to GAPDH.

CHAPTER 3

3 Results and Discussion

3.1 Polymer Synthesis and Characterization

Initially, synthesis of another poly (ester amide) consisting of L-phenylalanine (P), 1,4-butanediol (B) and sebacoyl chloride (Se) was attempted. Although this polymer named PBSe was successfully synthesized, it did not dissolve in a variety of organic solvents for electrospinning and hence was not considered further. Due to this, efforts were made to synthesize another poly (ester amide) from L-alanine (A), 1,8-octanediol(O) and sebacoyl chloride (Se). It was obtained by interfacial polymerization following the scheme outlined in Figure 1. L-alanine was chosen because of its short side chain which subsequently contributes to crystallinity. 1, 8-octanediol was chosen due to its long carbon chain, which in turn provides flexibility.

Interfacial polymerization was chosen due to several reasons. Firstly, restrictions on purity and stoichiometry are not as rigid and, a common solvent for both monomers is not necessary. This allows for the formation of high molecular weight polymers on the interface of the two solutions. Secondly, because the reaction was carried out at a low temperature, high rates of reaction overcome any potential for side reactions to occur. This way, linear polymers of high molecular weights can be synthesized. Polymerization times were also significantly reduced compared with solution polymerization times.[84]

3.1.1 Structural Analysis

The structures of the polymers were confirmed by ^{1}H-NMR and FT-IR spectra. Figures 2 and 3 show the ^{1}H-NMR spectra for polymers PBSe and AOSe respectively.

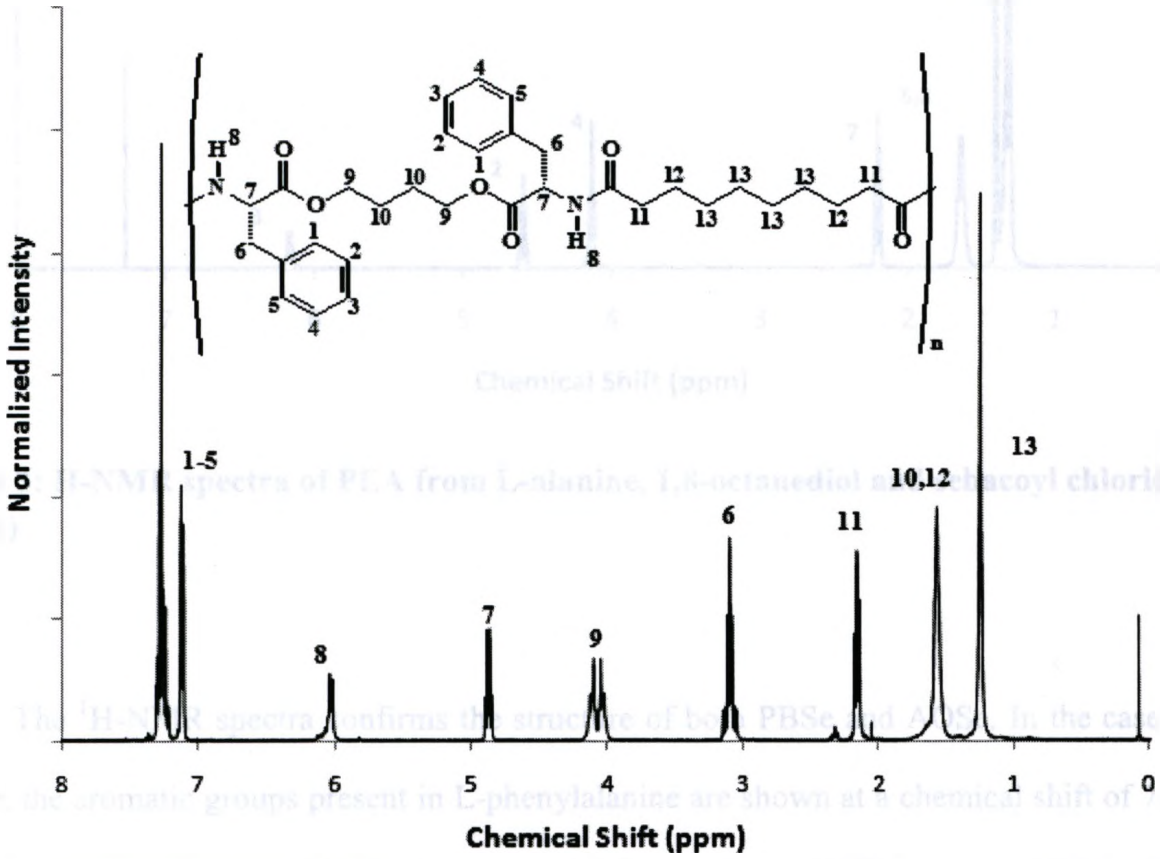

Figure 2:^{1}H-NMR spectra of PEA from L-phenylalanine, 1,4-butanediol and sebacoyl chloride (PBSe)

Structure is confirmed by peaks obtained and are labelled from 1-9. Due to the aliphatic nature of L-alanine, no aromatic peak is observed at 7ppm as compared to Figure 2.

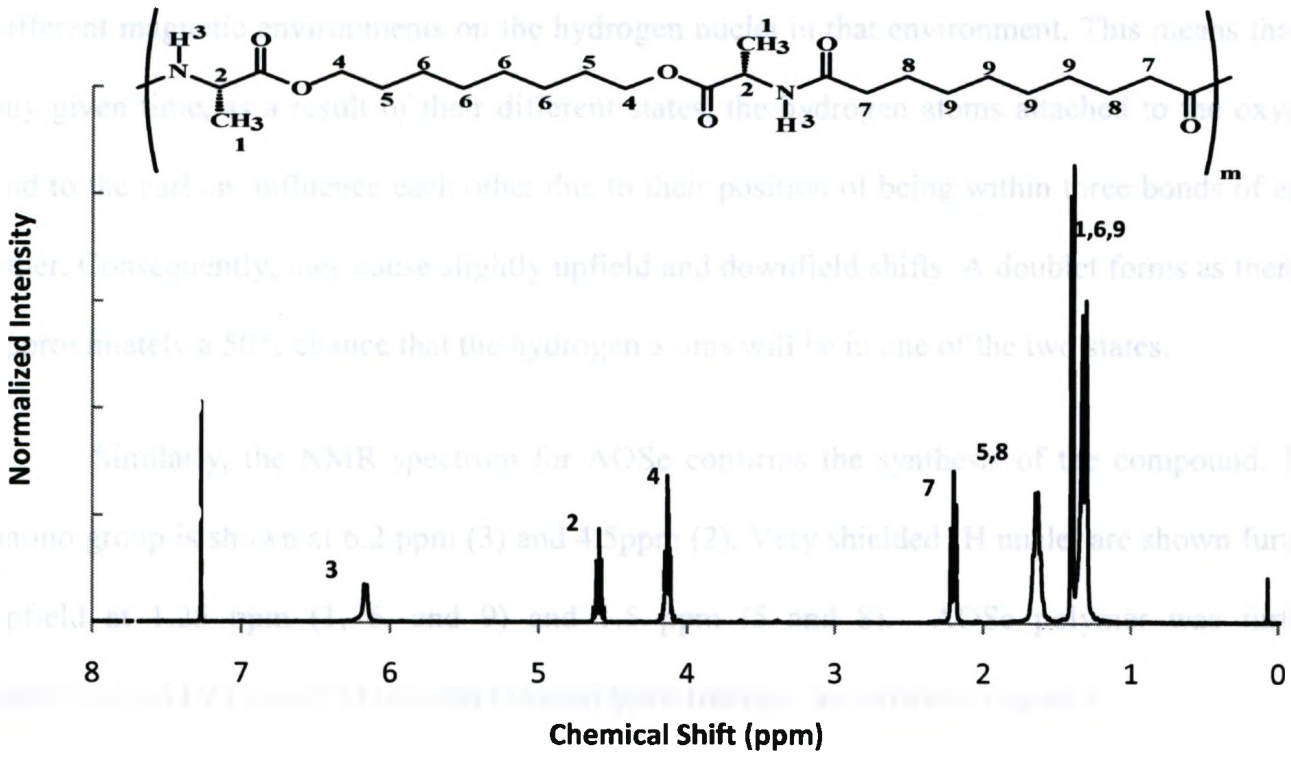

Figure 3: H-NMR spectra of PEA from L-alanine, 1,8-octanediol and sebacoyl chloride (AOSe)

The ^{1}H-NMR spectra confirms the structure of both PBSe and AOSe. In the case of the former, the aromatic groups present in L-phenylalanine are shown at a chemical shift of 7.2 ppm (1-5) and the amino group N-H at 6.01 ppm and 4.5 ppm (7 and 8). The reason that these groups are further downfield than the rest is due to the electron withdrawing nature of these bulky groups, where the electron cloud that normally surrounds the ^{1}H are pulled away from the nucleus, thus creating a de-shielding effect. De-shielding causes the hydrogen nucleus of these molecules to resonate at lower field intensity. Conversely, electron donating atoms such as the carbons present in the methyl groups shield the nuclei, thus creating a tightly bound electron

cloud and therefore presenting an upfield position on the spectra, indicated by numbers 10 and 12 at 1.5 ppm and 13 at 1.25 ppm. Splitting occurs at 9, at 4ppm, due to the presence of two different magnetic environments on the hydrogen nuclei in that environment. This means that at any given time, as a result of their different states, the hydrogen atoms attached to the oxygen and to the carbon, influence each other due to their position of being within three bonds of each other. Consequently, they cause slightly upfield and downfield shifts: A doublet forms as there is approximately a 50% chance that the hydrogen atoms will be in one of the two states.

Similarly, the NMR spectrum for AOSe confirms the synthesis of the compound. The amino group is shown at 6.2 ppm (3) and 4.5ppm (2). Very shielded ^{1}H nuclei are shown further upfield at 1.25 ppm (1, 6, and 9) and 1.5 ppm (5 and 8). AOSe polymer was further characterized by Fourier Transform Infrared Spectroscopy, as shown in Figure 4.

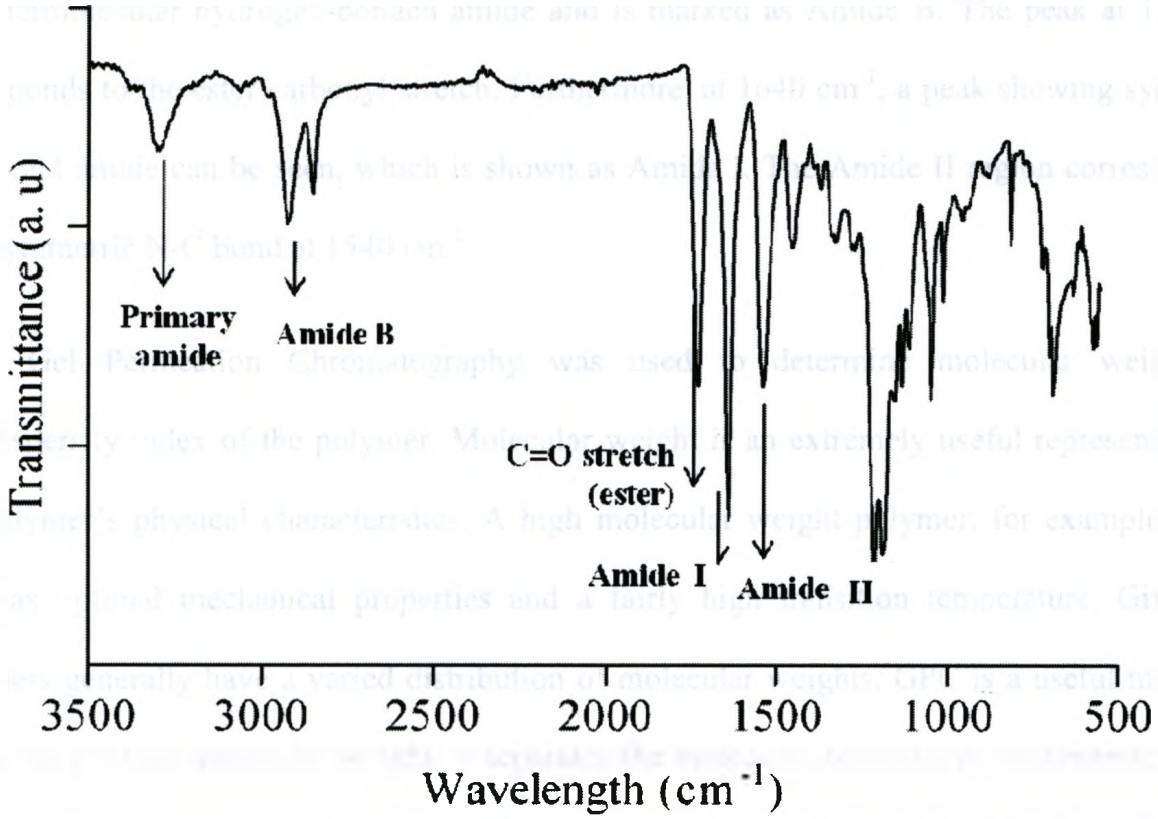

Figure 4: FT-IR of degradable AOSe PEA synthesized by interfacial polymerization

Note: Peak at 3300cm^{-1} shows primary amide, 2922cm^{-1} shows amide B. At 1730cm^{-1} is the carbonyl ester stretch and at 1640cm^{-1}, N-C bond amide as Amide I. The Amide II region is the asymmetric N-C bond at 1540cm^{-1}.

For FT-IR absorption, vibrations must result in a bond dipole moment in order for it to be recorded in the fingerprint region. Asymmetric bonds are clearly displayed in the spectra shown above. Bond stretching involves the largest change in energy and thus can be observed in the higher frequency regions between 3500 and 1500 cm^{-1}. Beyond this region, between 1500 and 400 cm^{-1}, vibrations generally constitute a combination of bending, stretching and rotating, and attributes to being the fingerprint region of the molecule. A strong primary amide absorption can be seen at 3300 cm^{-1} and can be classified as a sharp N-H stretch, as depicted in Figure 4. At

2922 cm^{-1}, a C-H_2 stretch is observed because of the aliphatic region of the amino acid; this is the intermolecular hydrogen-bonded amide and is marked as Amide B. The peak at 1730cm^{-1} corresponds to the ester carbonyl stretch. Furthermore, at 1640 cm^{-1}, a peak showing symmetric N-C bond amide can be seen, which is shown as Amide I. The Amide II region corresponds to the asymmetric N-C bond at 1540 cm^{-1}.

Gel Permeation Chromatography was used to determine molecular weight and polydispersity index of the polymer. Molecular weight is an extremely useful representation of the polymer's physical characteristics. A high molecular weight polymer, for example, is one that has optimal mechanical properties and a fairly high transition temperature. Given that polymers generally have a varied distribution of molecular weights, GPC is a useful method to assess the average molecular weight; it separates the molecules based on hydrodynamic volume and is therefore plotted as a function of elution volume. Figure 5 shows the GPC trace for AOSe PEA from which an average molecular weight of 32,000 g/mol and a polydispersity index of 1.56 were obtained. The yield for the PEA ranged from 80-85%.

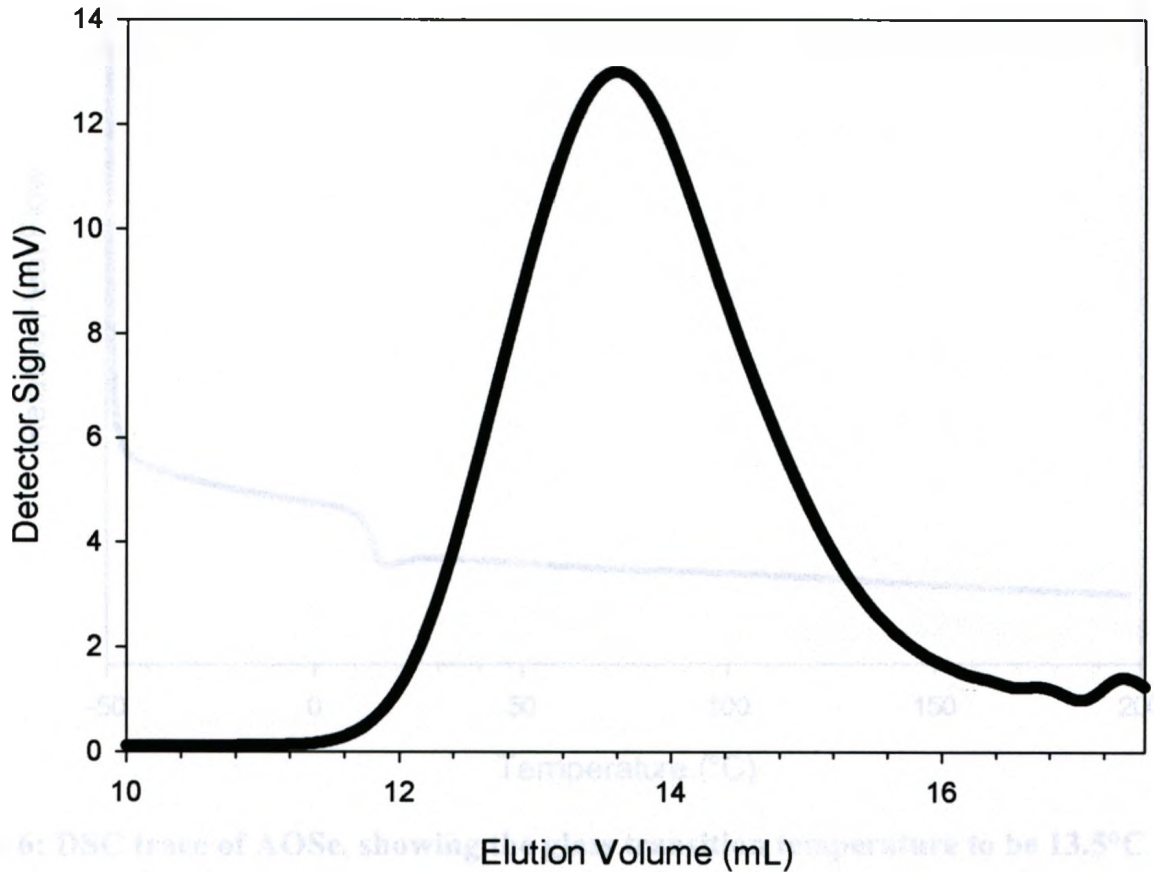

Figure 5: GPC trace of AOSe synthesised by interfacial polymerization

3.1.2 Thermal Analysis

In order to determine the glass transition temperature (T_g), DSC experiments were carried out. As it can be seen in Figure 6, the T_g is approximately 13.5°C. This relatively low temperature is probably due to the long carbon chains of 1,8-octanediol the ten carbon chain of sebacoyl chloride. In addition, there are no aromatic groups that allow for domination of transition temperature. There were no melting transitions during the second heating cycle.

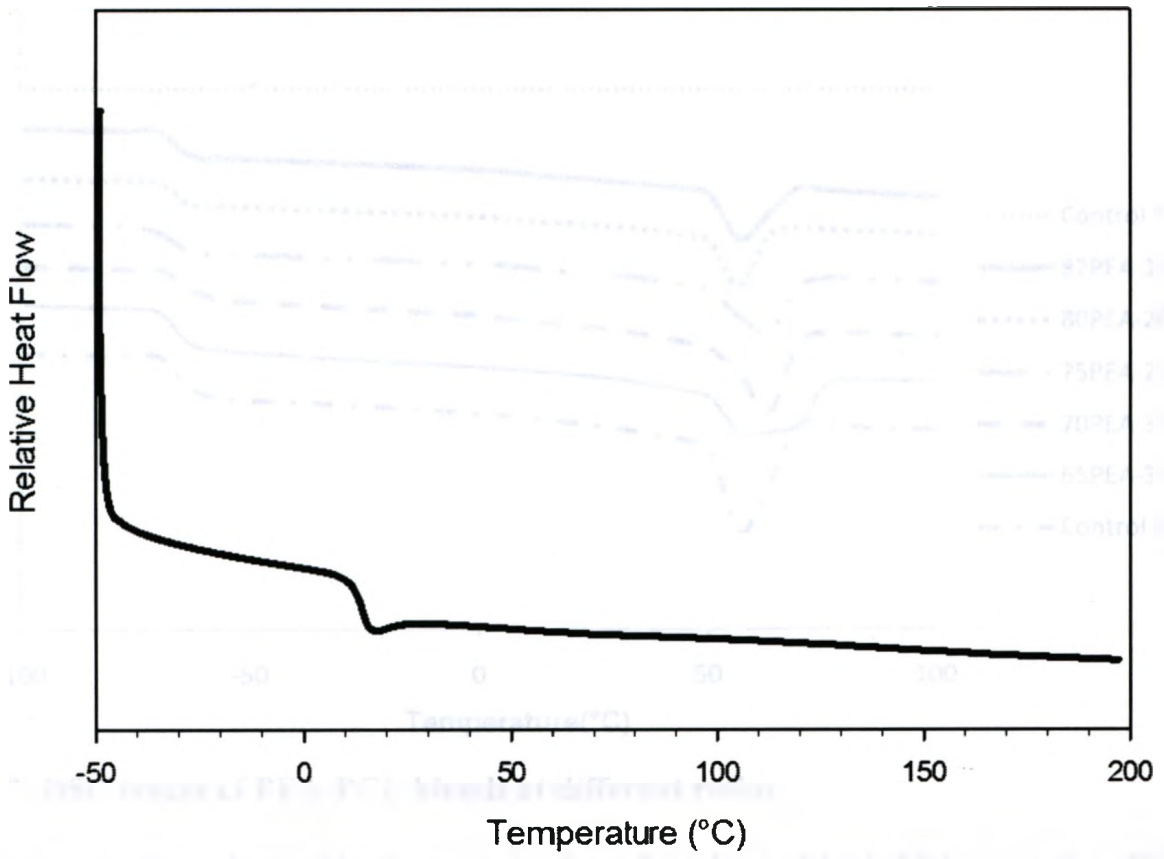

Figure 6: DSC trace of AOSe, showing the glass transition temperature to be 13.5°C

With regard to PCL, it has been confirmed from literature that the glass transition temperature is -60°C and the melting temperature is around 60°C. [85] It is also semi-crystalline due to its nature to pack very tightly. Polymer blends ranging from PEA: PCL ratios of 65:35 to 82:18 were prepared by heat-pressing into discs to analyze thermal property trends. The resulting curves are shown in Figure 7.

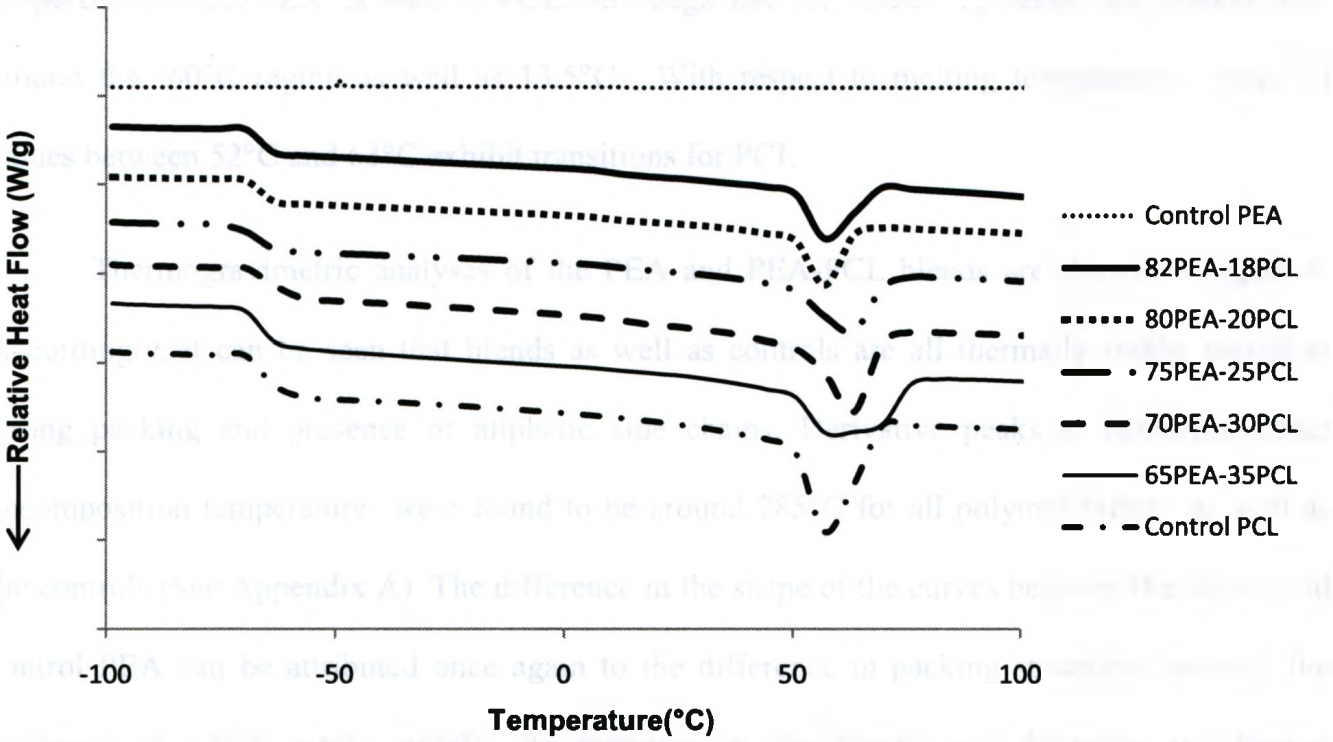

Figure 7: DSC traces of PEA-PCL blends at different ratios

As such, the polymer blends seem to show T_g values of both PEA as well as PCL. T_g values of PEA can be clearly seen on the 82PEA-18PCL curve, whereas it is not as apparent in the others. It is worth to notice that as PEA concentration increases, PCL properties may dominate. Due to a small increase in free volume, T_g values may reduce slightly. Glass transition temperatures of PCL seem to fluctuate between the ranges of -57 and -63°C throughout the different ratios of polymer blends. Based on packing densities and existing knowledge of PCL, it can be stated that the more percentage of PCL present in the polymer blend, the greater the value of the melting temperature, Tm. This can be attributed to the fact that more energy is required to overcome the cohesive forces, thereby increasing the overall melting temperature as well. For these blends, it can be seen from Figure 7 that they fluctuate between 52 and 63°C and in most cases, follow the above mentioned trend. However, only further in-depth studies about the thermal character of these blends can shed light on whether the curves are indeed following a trend or if it is simply a matter of statistical fluctuations. Polymer blends showed thermal

properties of both PEA as well as PCL. Although not very clear, T_g values are present both around the -60°C region as well as 13.5°C. With respect to melting temperatures, range of values between 52°C and 63°C exhibit transitions for PCL.

Thermogravimetric analyses of the PEA and PEA-PCL blends are shown in Figure 8. Accordingly, it can be seen that blends as well as controls are all thermally stable, owing to strong packing and presence of aliphatic side chains. Derivative peaks to determine onset decomposition temperatures were found to be around 285°C for all polymer blends, as well as the controls (See Appendix A). The difference in the shape of the curves between the blends and control PEA can be attributed once again to the difference in packing structures between the polymers. As PCL packs tightly, its presence in the blend may dominate its thermal characteristics although the blends seem to essentially exhibit aspects of both PEA as well as PCL.

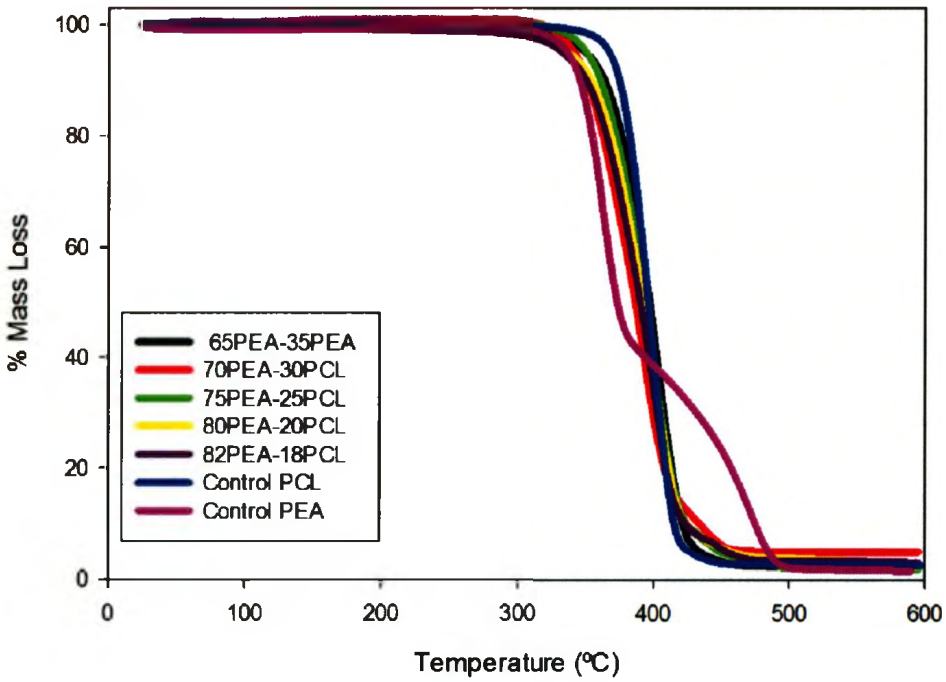

Figure 8: TGA traces of polymer blends and controls. Blends as well as polymer controls can be seen to be thermally stable. Onset decomposition temperature is around 285°C for all curves.

3.1.3 XRD Analysis

X-ray diffraction was carried out on both polymers as well as one polymer blend (70PEA-30PCL) and results are shown in Figure 9. From the curves obtained, it can be seen that all three samples are semi-crystalline.

PCL diffraction at 2θ values of 21.7° and 23.9° indicate peak maxima corresponding to a *d*-spacing of 0.415 nm and 0.384 nm respectively, which seems consistent with literature. [86] PEA showed strong diffraction patterns at an angle 2θ of 21.2°, which can be converted to a d-spacing of 0.412 nm. It is interesting to compare these values to the spectra of the polymer blend. The polymer blend, 70PEA-30PCL, shows strong diffractions at three different points and indicates

semi-crystallinity as well. Although the diffraction angles of 21.6° and 23.6° seem to mirror PCL maxima, the PEA peak has been shifted to 25.4° (d-spacing = 0.287 nm). Also, electrospun fibres of crystalline polymers usually are less crystalline than pure polymer powders due to solvent evaporation; as a result, the polymer blend peaks are not as pronounced. [86] This can be explained by the stretching of fibres during electrospinning as well as the evaporation of the solvent, which both occur so fast that the polymer chains are not allowed sufficient time to crystallize completely.[86] In addition, it can be seen that all the minor peaks associated with both the polymer controls are depicted in the polymer blend, namely at diffraction angles of 29.2°, 35.1° and 39.6°. Once again, the peaks from PEA seem to have shifted slightly when compared to their position on the polymer blend spectra. This can be attributed to the domination of PCL packing over PEA, and therefore exhibits no shifts in peaks.

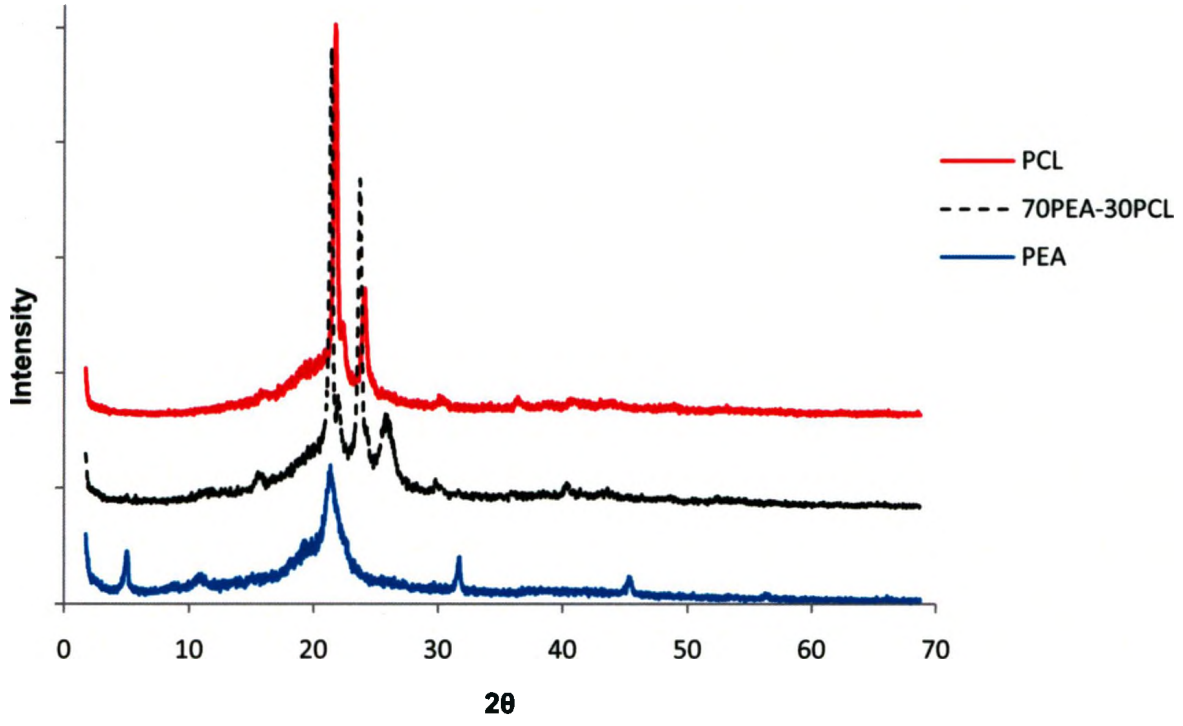

Figure 9: XRD Spectra of PEA, PCL and 70PEA-30PCL. Peaks as reported in literature can be observed for PCL at 21.7° and 23.9°.[86] PEA maximum occurs at 2θ value of 21.2°. 70PEA-30PCL polymer blend shows diffraction peaks at 21.6°, 23.6° and 25.4°.

3.2 Electrospinning

Despite its difficulty to dissolve in many organic solvents, attempts to electrospin PBSe using dimethylsulfoxide (DMSO) as a solvent was carried out. However, this was not pursued further due to the fact that DMSO's high boiling point meant that the solvent did not completely evaporate upon reaching the collector and, therefore, the polymer solution re-dissolved after reaching the collector. Even after drying the samples in vacuum overnight, no fibres were observed. PBSe in concentrations greater than 5% w/w was not soluble in DMSO or any other organic solvent and, hence, limited its utility.

PEA based on AOSe was then successfully synthesized as it is a readily soluble in chloroform up to 35% w/w. At this concentration, the solution was not however viscous enough for electrospinning. In order to increase the viscosity such that it can be electrospun, PCL was added as a viscosity modifier. PCL was chosen due to its commercial availability, biodegradability and previously published results showing its application in the field of biomedical engineering. [39] The amount of PCL added to the PEA was varied from 18% to 35% PCL. A minimum of 18% was required to electrospin the solution while the upper limit was set in order to limit the influence of PCL on the electrospun fibres.

Sample nomenclature is based on the weight percentage of the PEA and PCL used in the preparation. For example, 65PEA-35PCL means an electrospun fibre mat from 65 wt% PEA and 35 wt% PCL. Accordingly, five compositions namely, 65PEA-35PCL, 70PEA-30PCL, 75PEA-25PCL, 80PEA-20PCL and 82PEA-18PCL were prepared and electrospun. Figure 10 shows representative SEM micrographs of electrospun mat spun at different solution concentration and needle-to-collector distances. It can be seen that the fibres are randomly oriented and are reasonably uniform in sizes with no beading effect.

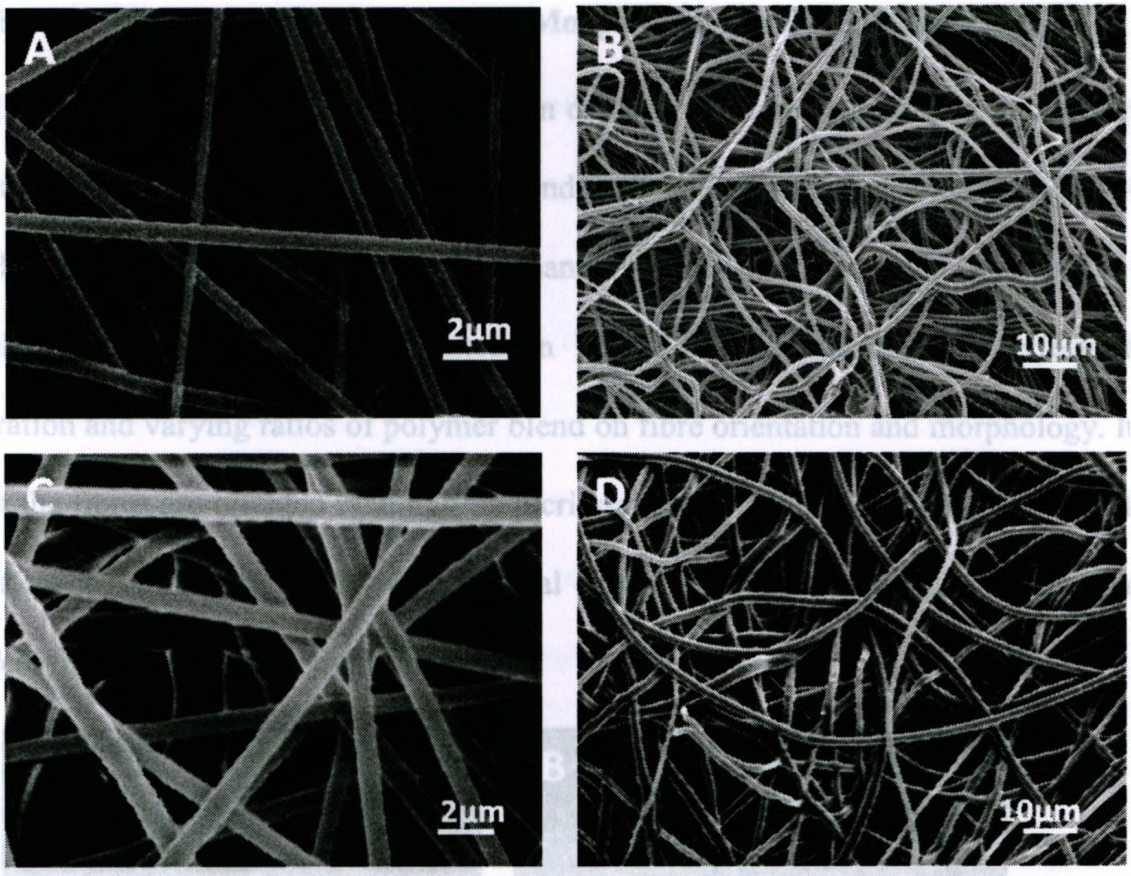

Figure 10: SEM images of different electrospun mats at different magnifications, concentrations and distances to collector. Fibres were electrospun at 13kV and flow rate of 0.08mL/h. 70PEA-30PCL (14%w/w) at 8cm (A) and 14cm ;(B) 82PEA-18PCL (21.5%w/w) at 8cm (C) and 14cm (D)

3.2.1 Electrospinning Parameters

There are several parameters governing the process of electrospinning. These are flow rate of the solution through the needle, voltage, polymer concentration, distance to collector and solution conductivity. Typically, most of these parameters are kept constant while some are varied to achieve the optimum results. For this study, two parameters namely, the polymer concentration and the distance to collector, were studied in depth. SEM was used to characterize the electrospun mats and ImageJ software was used to measure fibre diameters at different concentrations, ratios and distances; pore size distributions were also studied for specific concentrations.

3.2.2 Effect of Polymer Concentration on Morphology and Fibre Diameter

In this study, the effect of concentration on fibre diameter was studied in two ways. Due to the experimental setup for each polymer blend, both solution concentration (namely, 14%w/w to 21.5%w/w), and PEA: PCL ratio are changing thus each parameter had to be studied separately. A panel of images presented in Figure 11 demonstrates the effects of both concentration and varying ratios of polymer blend on fibre orientation and morphology. It can be seen that the fibres are oriented randomly in a criss-crossing grid-like pattern. This orientation is desirable, as it mimics the actual physiological structure of the extracellular matrix and could prove ideal for *in vitro* tissue engineering.

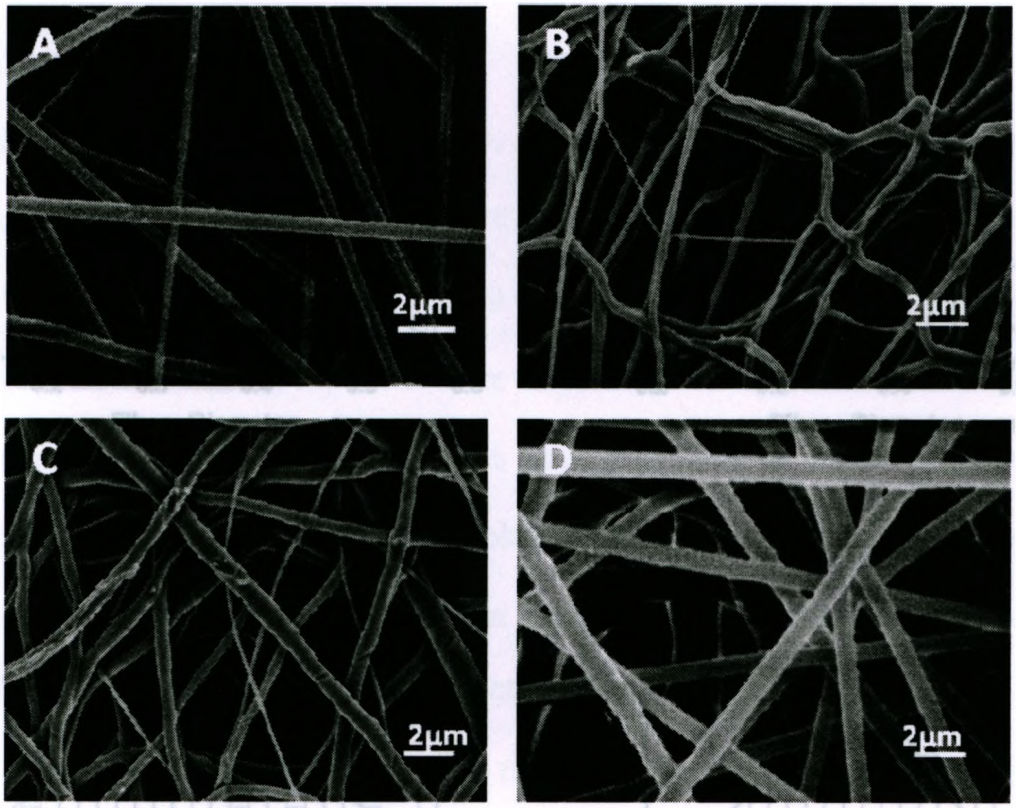

Figure 11: SEM images of electrospun mats at varying concentrations and compositions. Electrospun at 8cm, 13kV and flow rate 0.08mL/h. A) 70PEA-30PCL, 14% w/w; B) 75PEA-25PCL , 16.5% w/w; C) 80PEA-20PCL, 19% w/w; D) 82PEA-18PCL , 21.5% w/w.

In order to systematically study the underlying parameter affecting changing fibre diameter, the role of the polymer ratios was studied. This was accomplished by keeping the final solution concentration constant at 14%w/w and by manipulating the polymer composition at 70PEA-30PCL, 75PEA-25PCL, 80PEA-20PCL and 82PEA-18PCL. Pure PCL was used as a control. As mentioned earlier, PEA could not be electrospun on its own, as a result, only the presence of one control was made possible. These set of experiments were also conducted for another concentration namely, 19%w/w. Figure 12 demonstrates the fibre distribution for different polymer blends at 14% concentration whereas Figure 13 presents the effect of varying polymer composition on the resulting fibre diameter.

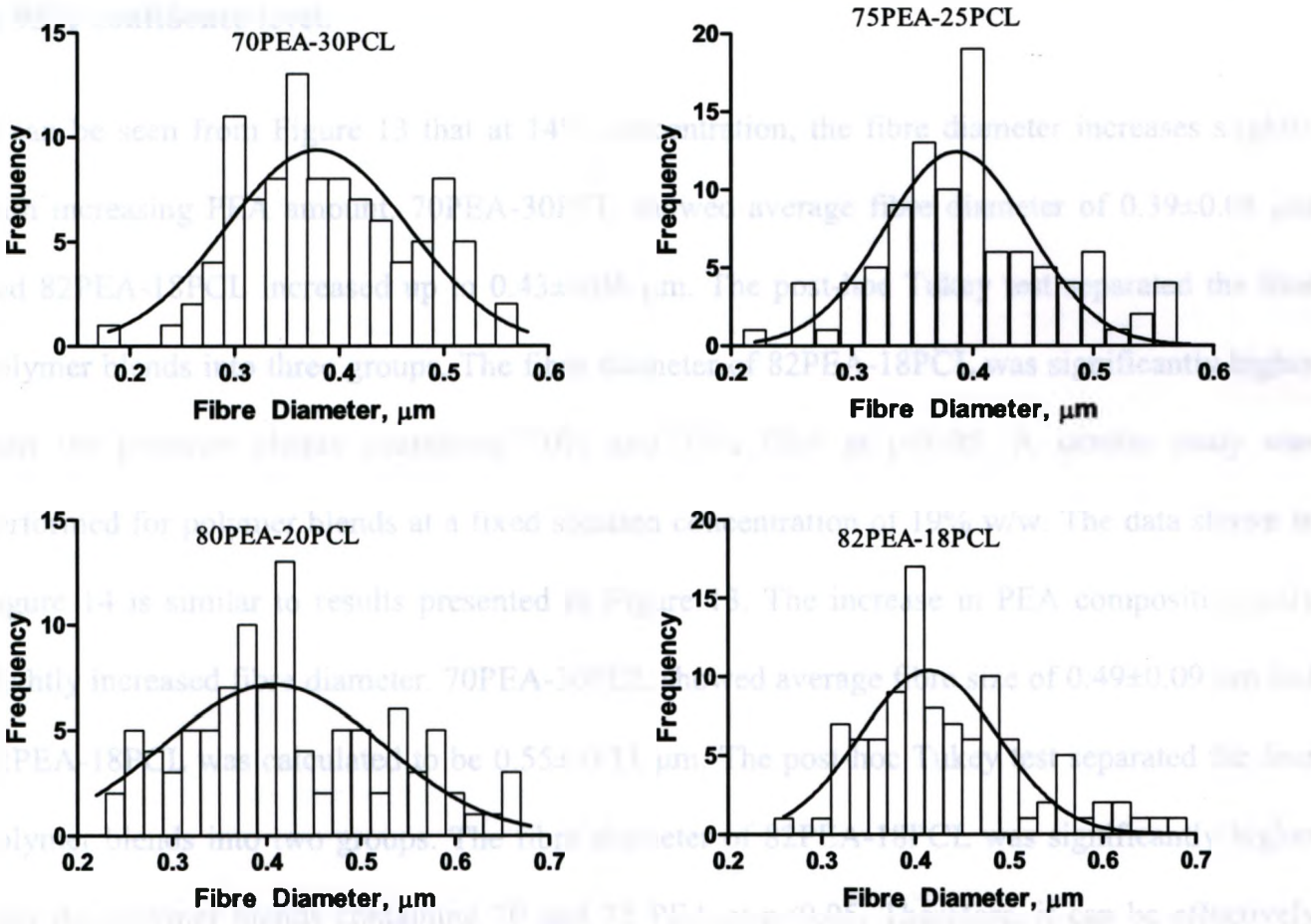

Figure 12: Frequency distribution of electrospun fibre diameter showing the effect of polymer blend ratios at a fixed concentration of 14%w/w. The voltage was 13kV and the distance to collector was 8cm.

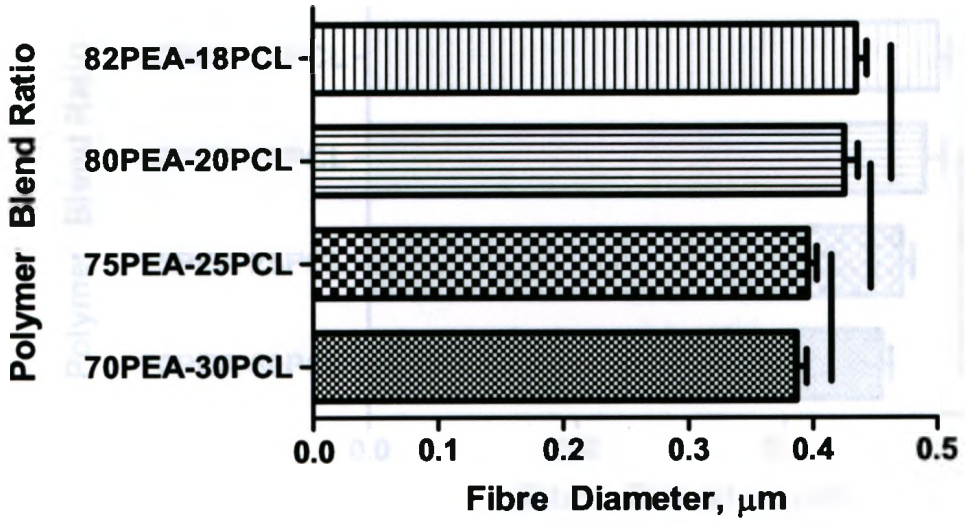

Figure 13: Fibre diameter for different polymer blend ratios at solution concentration of 14%w/w. Solid lines indicate that data sets are not significantly different from each other at 95% confidence level.

It can be seen from Figure 13 that at 14% concentration, the fibre diameter increases slightly with increasing PEA amount. 70PEA-30PCL showed average fibre diameter of 0.39±0.08 μm and 82PEA-18PCL increased up to 0.43±0.06 μm. The post-hoc Tukey test separated the four polymer blends into three groups. The fibre diameter of 82PEA-18PCL was significantly higher than the polymer blends containing 70% and 75% PEA at $p<0.05$. A similar study was performed for polymer blends at a fixed solution concentration of 19% w/w. The data shown in Figure 14 is similar to results presented in Figure 13. The increase in PEA composition only slightly increased fibre diameter. 70PEA-30PCL showed average fibre size of 0.49±0.09 μm and 82PEA-18PCL was calculated to be 0.55± 0.11 μm. The post-hoc Tukey test separated the four polymer blends into two groups. The fibre diameter of 82PEA-18PCL was significantly higher than the polymer blends containing 70 and 75 PEA at $p<0.05$. Therefore, it can be effectively concluded that fibre diameter is not affected by the composition of the polymer blends at constant concentration,

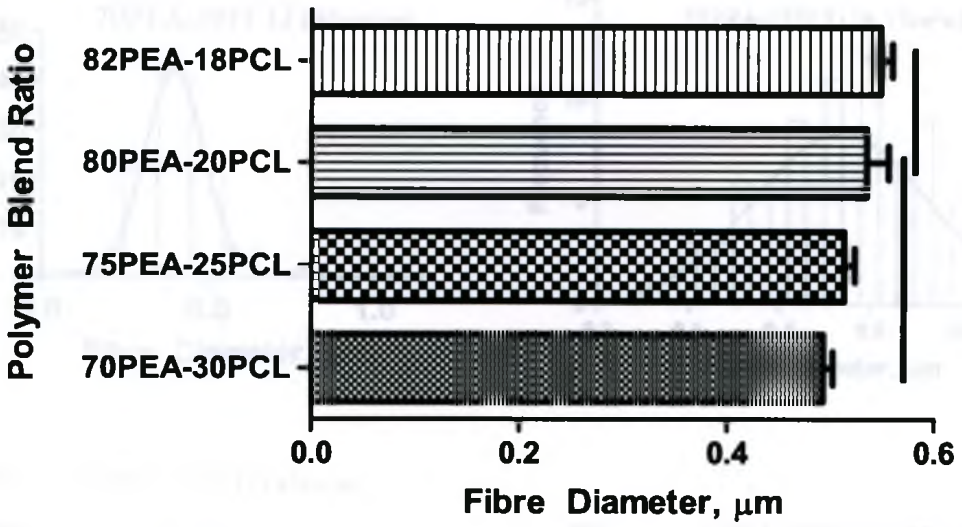

Figure 14: Fibre diameter for different polymer blends at solution concentration of 19%w/w. Solid lines indicate that data sets are not significantly different from each other at 95% confidence level.

The effect of solution concentration on fibre diameters is presented in Figures 15 and 16. Figure 15 shows the frequency distribution and Gaussian curve fit for each concentration. Figure 16 demonstrates the relationships between increasing concentrations in the range of 14%w/w to 21.5%w/w and resulting fibre diameter. It can be seen that concentration does in fact, have an effect on fibre diameter where an increase in solution concentration increased the fibre diameter. Average fibre size for 70PEA-30PCL was calculated to be 0.41±0.13 μm and 82PEA-18PCL showed fibre diameters of 0.81±0.39 μm. The post-hoc comparative Tukey test separated five different concentrations into four significant groups at $p<0.05$. It can be inferred from Figure 16 that the trend is consistent with literature. [79, 81, 83]

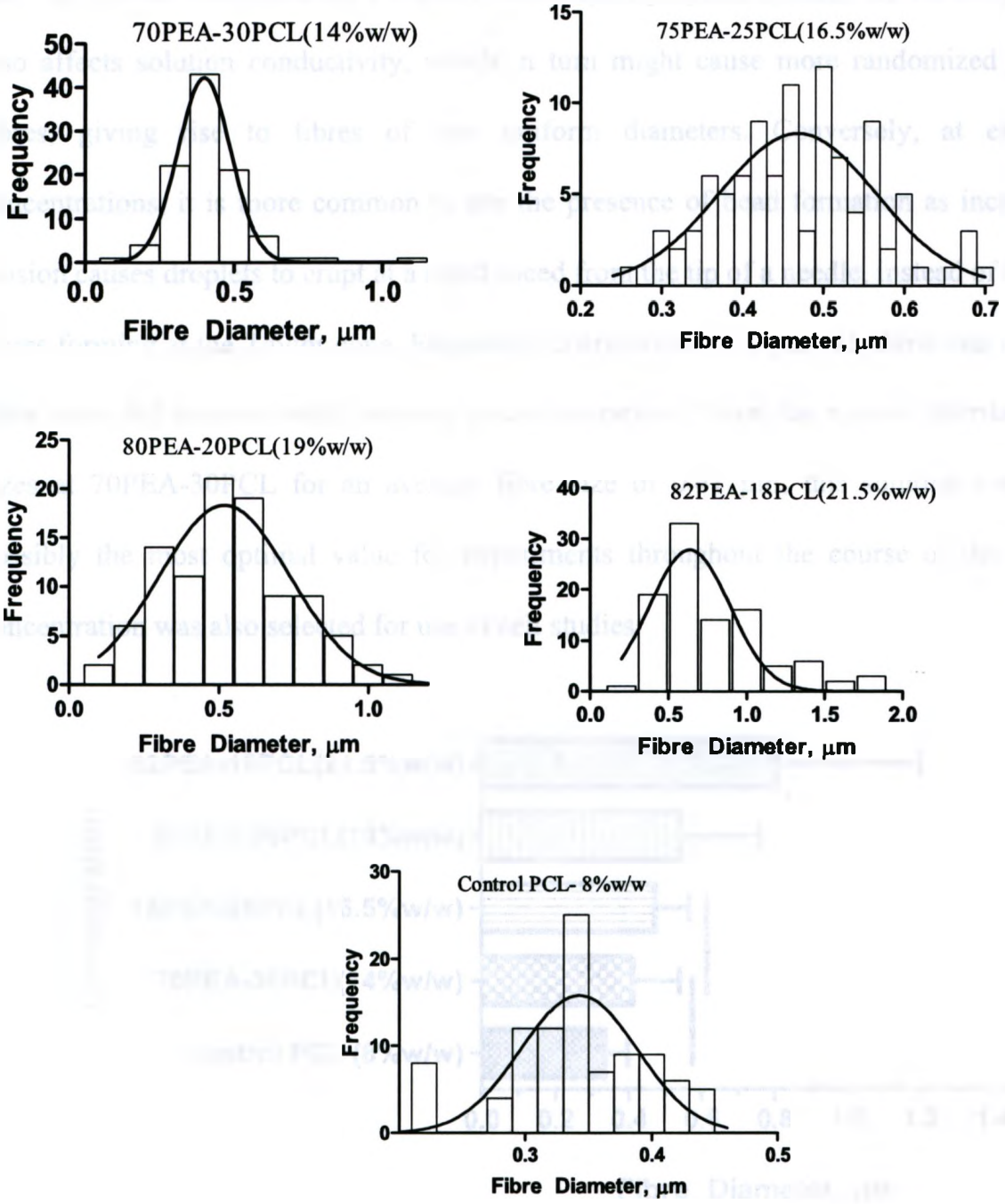

Figure 15: Frequency distribution of fibre diameters of varying concentrations

Increase in fibre size can generally be attributed to the fact that as solution viscosity increases, the amounts of polymer present in the solution also increases, thus forming a thicker jet before deposited at the collector. However, the data also shows that the standard deviation of the fibre diameter significantly increases with increasing concentration. This is evidence that there is in

fact, an optimal concentration for every electrospun polymer system. As viscosity increases, it also affects solution conductivity, which in turn might cause more randomized deposition of fibres, giving rise to fibres of less uniform diameters. Conversely, at extremely low concentrations, it is more common to see the presence of bead formation as increased surface tension causes droplets to erupt at a rapid speed from the tip of a needle, instead of a steady jet of fibres forming at the Taylor cone. Frequency distributions in Figure 15 show that distribution of fibre sizes did increase with increase in concentration. Given the narrow distribution of fibre sizes at 70PEA-30PCL for an average fibre size of 0.41 μm, this solution concentration is possibly the most optimal value for experiments throughout the course of the project. This concentration was also selected for use in cell studies.

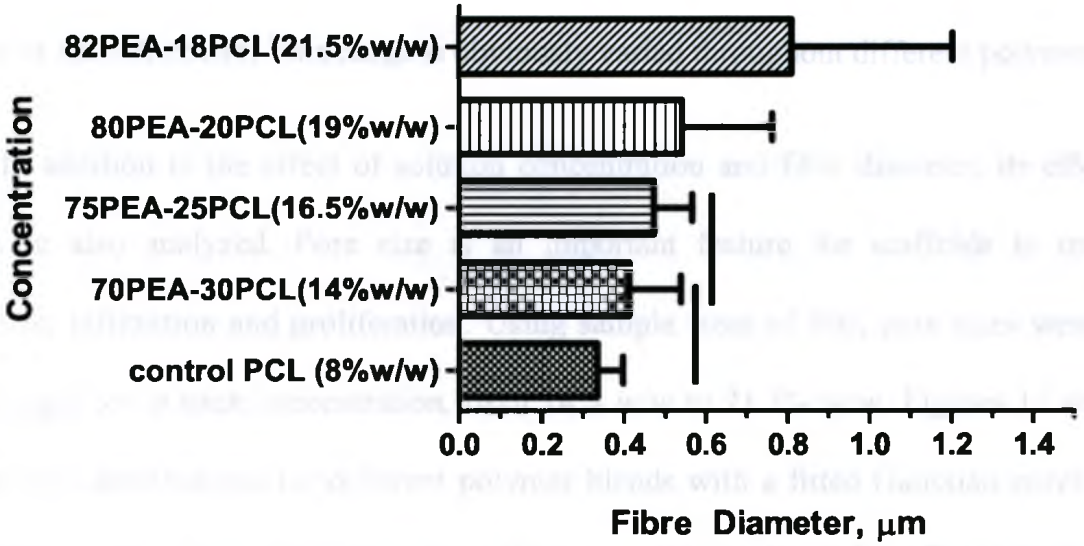

Figure 16: Fibre diameter for different solution concentrations. Solid line indicates that data is not statistically significant at 95% confidence level.

The effect of viscosity on the electrospun fibre size has been studied extensively and has been demonstrated to be a significant variable. Typically, at low concentrations, a phenomenon known as beading occurs due to increased surface tension at the tip of the needle.[79-81]

Increasing solution concentration yields more uniform fibres with fewer beads; however, this is only up to a certain viscosity. If this value is too high, i.e, the solution concentration was raised beyond the optimum range, the droplet dried out at the tip before a steady jet of fibres could be formed.[81, 87, 88] In the extreme case where the viscosity is too high, electrospinning is not possible as the solution will not be able to move through the needle even if the flow rate is significantly increased. There seems to be a direct correlation between intrinsic viscosity [η], concentration (*c),* and final fibre size for a particular polymer solution system. These correlations are highly system-dependent rather than universal. For example, for electrospinning poly(vinyl alcohol) (PVA) $[\eta]c > 5$ was reported to be essential.[81, 89] On the other hand, $[\eta]c$ value higher than 10 was needed for a system consisting of poly(ethylene terephthalate) (PET).[90] Overall, it can be concluded that increasing solution concentration within an optimum range results in the increase in fibre diameter. This range is obviously varied throughout different polymer systems.

In addition to the effect of solution concentration and fibre diameter, its effect on pore sizes were also analyzed. Pore size is an important feature for scaffolds to improve cell attachment, infiltration and proliferation. Using sample sizes of 100, pore sizes were measured using ImageJ for at each concentration, from 14% w/w to 21.5% w/w. Figures 17 and 18 show the pore size distributions for different polymer blends with a fitted Gaussian curve at varying concentrations as well as the average pore sizes respectively. It can be inferred from the figures that pore size is dependent on fibre diameter and consequently, on polymer solution concentration. With an increase in fibre diameter, pore size also increased. An obvious conclusion that can be made is that increasing fibre diameters and pore size would consequently result in a decrease in pore areas of the electrospun mat. Figure 18 shows that the average pore size depended on the polymer ratio used. Control PCL mats showed significantly smaller pores

than the PEA-PCL blends under otherwise identical electrospinning conditions. Figure 17 shows that the average pore size increased from 8.01±1.29 μm for 70PEA-30PCL (14% w/w) to 20.92±2.84 μm for 82PEA-18PCL (21.5% w/w). The post hoc Tukey multiple comparative test separated the five polymer systems displayed in Figure 18 into five significant groups at $p<0.05$.

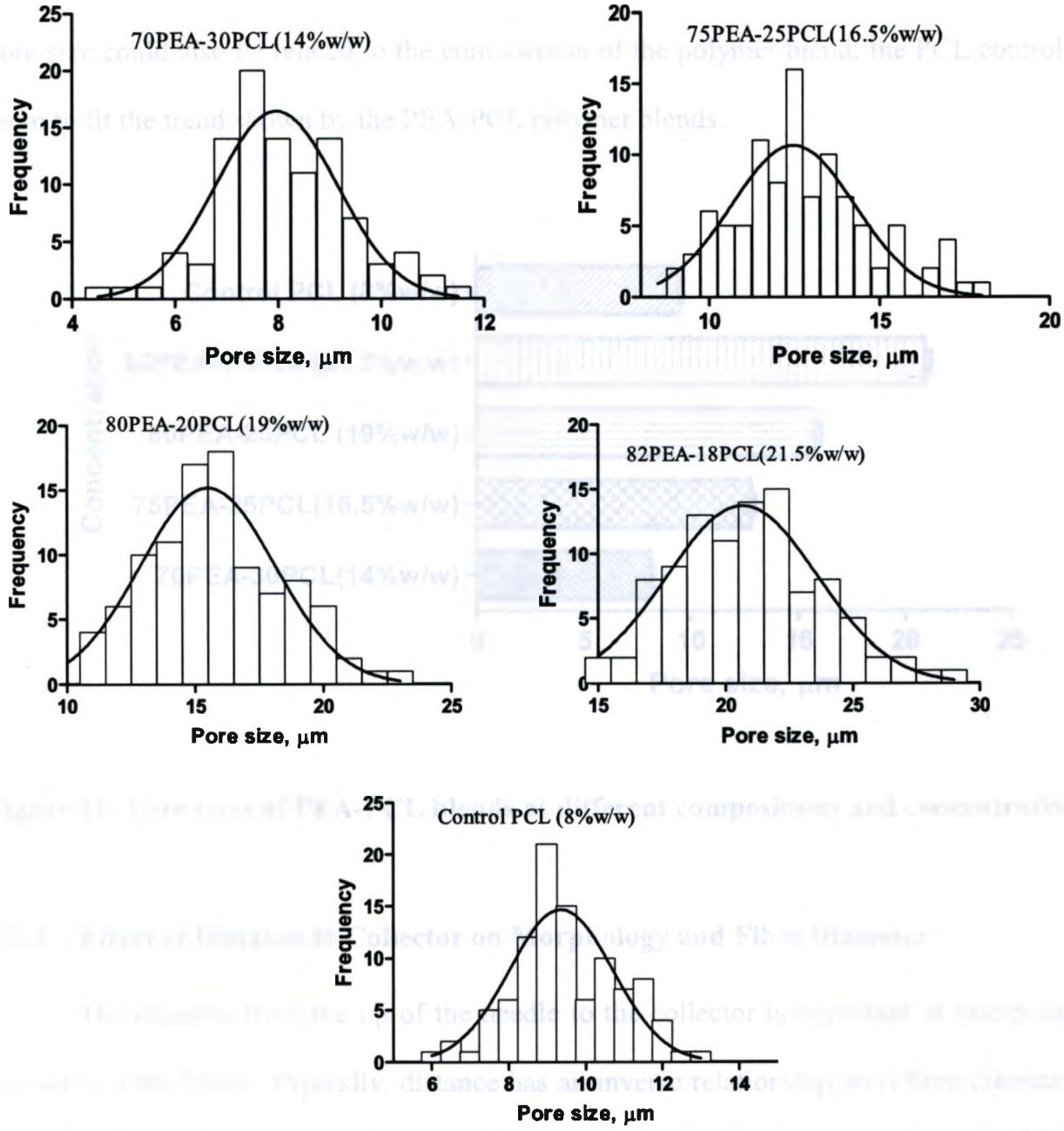

Figure 17: Frequency distribution of pore sizes showing the effect of varying concentrations for PEA-PCL blends.

It can, therefore, be concluded that solution concentration is an important parameter in the electrospinning process since the two polymer ratios did not significantly affect the fibre diameter. It was shown that polymer concentration was in fact responsible for the increase in fibre diameter, due to the formation of a thicker jet at the Taylor cone. In addition, pore size is directly related to fibre diameter; increasing fibre size leads to an increase in pore size. However, pore size could also be related to the composition of the polymer blend; the PCL control did not seem to fit the trend shown by the PEA-PCL polymer blends.

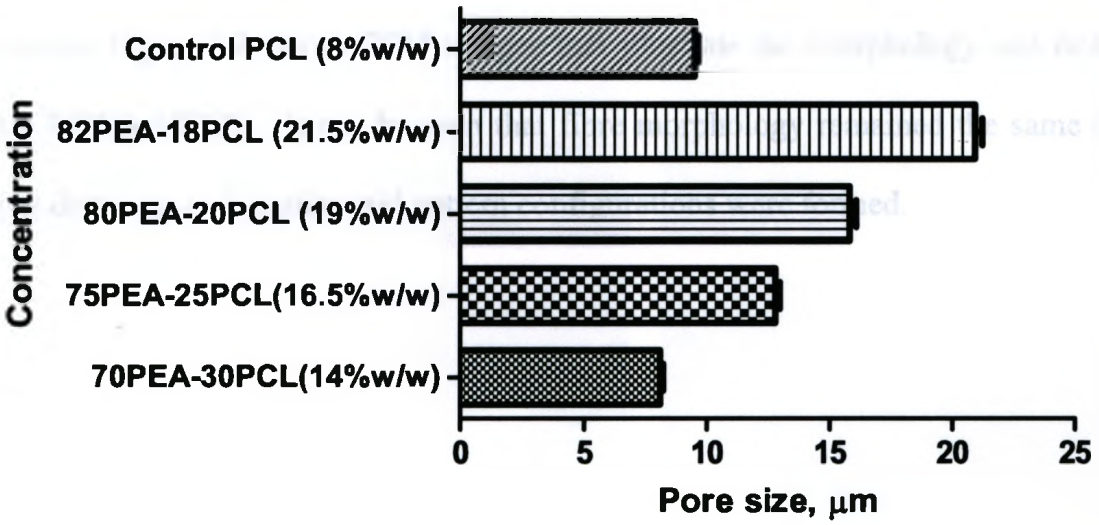

Figure 18: Pore sizes of PEA-PCL blends at different compositions and concentrations

3.2.3 Effect of Distance to Collector on Morphology and Fibre Diameter

The distance from the tip of the needle to the collector is important in manipulating the diameter of the fibres. Typically, distance has an inverse relationship with fibre diameter. It has been shown that with increasing distance, a decrease in fibre diameter was observed.[80, 81, 91] This is mainly due to the fact that as distance is increased, the fibres are allowed to stretch out more

before they are deposited on the collector. This ensures a uniform network of fibres that allows for smaller diameters.

However, as in the case of solution concentration, fibre diameters are affected by distance for a specific range and for a defined set of polymer systems. It has been reported in various studies that a minimum distance is needed for every electrospun scaffold in order to obtained dried fibres. [79-81, 83] At distances either too close or too far, beading was observed. To study the effect of distance, four distances, namely 8cm, 10cm, 12cm and 14cm from the collector were chosen. Other parameters were kept constant and samples were spun at 13kV, 0.08mL/h at 14% concentration. Figure 19 shows SEM images that illustrate the morphology and orientation of fibres for 70PEA-30PCL. It can be seen that fibre morphology remained the same despite the increasing distances and similar grid pattern configurations were formed.

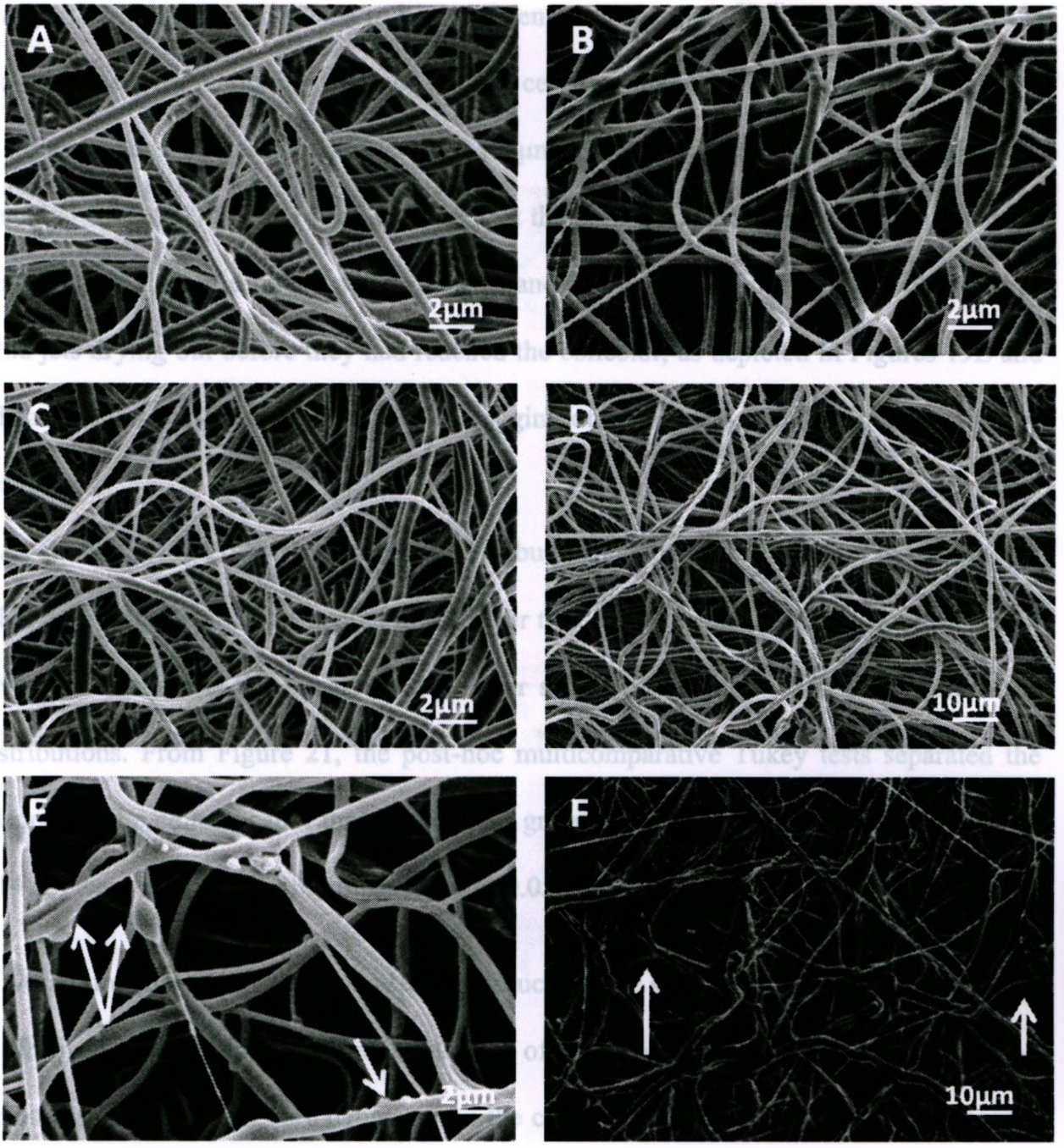

Figure 19: : SEM images of 70PEA-30PCL mats electrospun at 0.08mL/h and 13kV (A) 8cm (B) 10cm (C) 12cm and (D) 14cm (E) beading at 12cm and (F) beading at 14cm

To quantify the effect of distance, diameters of fibres (n=100) were measured at the four different distances. Frequency distribution plots and a bar diagram showing the relationship between fibre diameter and distance from the collector are displayed in Figures 20 and 21

respectively. The general trend seems to be consistent with literature,[81, 91] and fibre diameter is shown to decrease with increasing distance up to a certain point. Between 8 cm and 10 cm, the average fibre diameter decreased from 0.41± 0.13 μm to 0.37±0.09 μm then increased beyond 10cm reaching 0.47±0.09 μm at 14cm, showing that the optimal distance is probably from about 6-10cm away from the collector. In addition, at 12 and 14 cm, a lot of beading was observed as well as the jets drying out before they had reached the collector, as depicted in Figures 19E and 19F (indicated by arrows). This in turn led to clogging of fibres at the needle tip at the time of the experiment.

As shown in Fig 20 by the frequency distributions, Gaussian distribution is smooth and unvaried at 8 cm and 10 cm as compared to the other two distances. Specifically, at a distance of 10cm, average diameter is the lowest with a lower standard deviation when compared to the other distributions. From Figure 21, the post-hoc multicomparative Tukey tests separated the four distances to the collector into three significant groups at $p<0.05$. The fibre diameters at 12 cm and 14 cm were not significantly different at $p>0.05$.

Overall, the distance from the collector produced some significant results with respect to average fibre diameter. Due to added stretching of the fibres between the needle tip and collector, lower fibre diameters are deposited on the collector. However, this study also showed that this holds true only for a certain range of values, after which beading, clogging and increased fibre diameter were all observed.

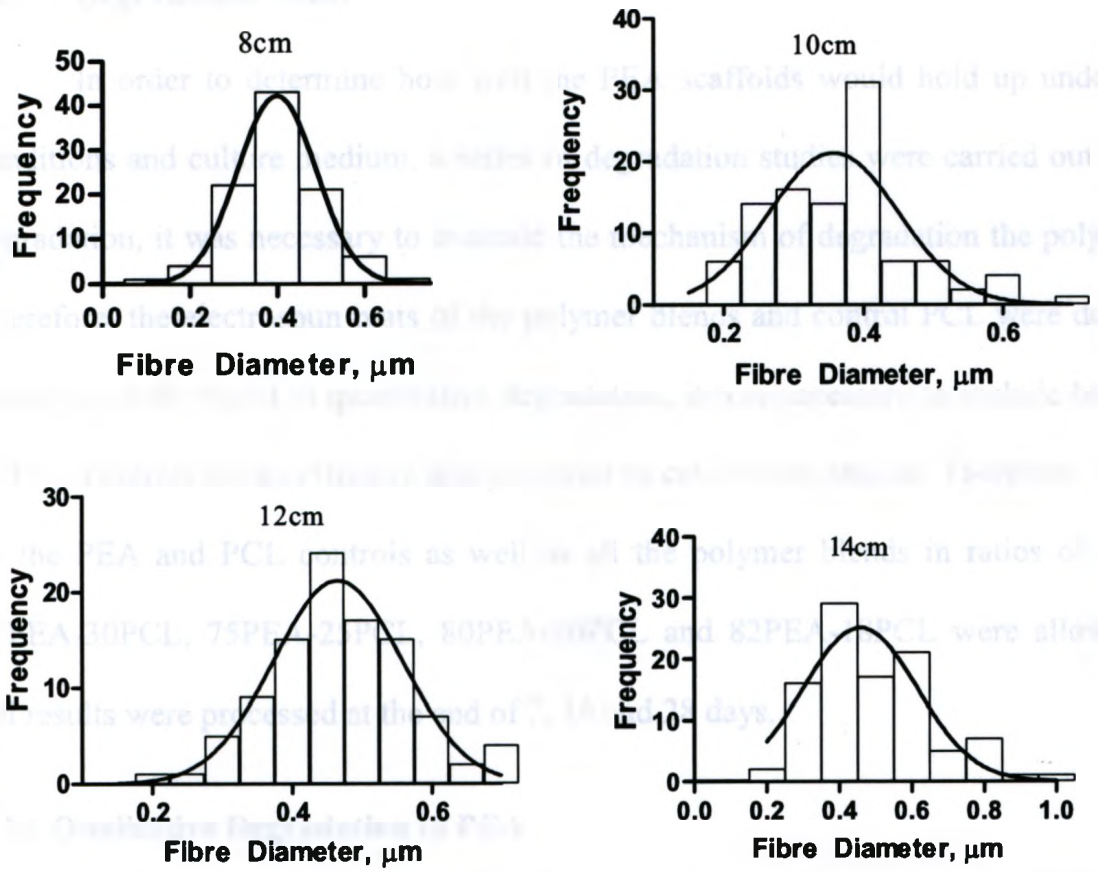

Figure 20: Frequency distribution of fibre diameters at varying distances from collector

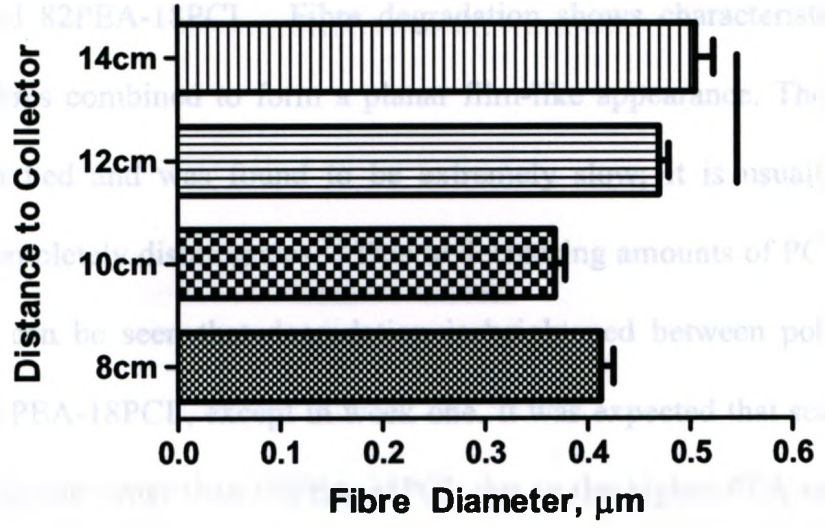

Figure 21: Average fibre diameter at different distances from the collector .Solid line indicates data sets are not statistically significant at a 95% confidence level.

3.3 Degradation Study

In order to determine how well the PEA scaffolds would hold up under physiological conditions and culture medium, a series of degradation studies were carried out. For qualitative degradation, it was necessary to evaluate the mechanism of degradation the polymer undergoes. Therefore, the electrospun mats of the polymer blends and control PCL were degraded in PBS. However, with regard to quantitative degradation, it was necessary to include both PEA as well as PCL controls for an effective analysis prior to cell culture studies. Therefore, all samples, that is, the PEA and PCL controls as well as all the polymer blends in ratios of 65PEA-35PCL, 70PEA-30PCL, 75PEA-25PCL, 80PEA-20PCL and 82PEA-18PCL were allowed to degrade. All results were processed at the end of 7, 14 and 28 days.

3.3.1 Qualitative Degradation of PEA

Figure 22 shows SEM images of electrospun polymer blend mats in PBS after 1, 2 and 4 weeks of degradation. Three different concentrations are shown, 65PEA-35PCL, 70PEA-30PCL and 82PEA-18PCL. Fibre degradation shows characteristics of fibre fusing, where adjacent fibres combined to form a planar film-like appearance. The degradation rate of PCL has been studied and was found to be extremely slow; it is usually about 2 years before a scaffold completely disintegrates.[92] Due to decreasing amounts of PCL and increasing quantities of PEA, it can be seen that degradation is heightened between polymer blend of 65PEA-35PCL and 82PEA-18PCL, except in week one. It was expected that scaffolds made of 82PEA-18PCL will degrade faster than 65PEA-35PCL due to the higher PEA content of the former. Fibre meshing and fusing increased as the degradation time increased and these can be visualized in the SEM images in Figure 22.

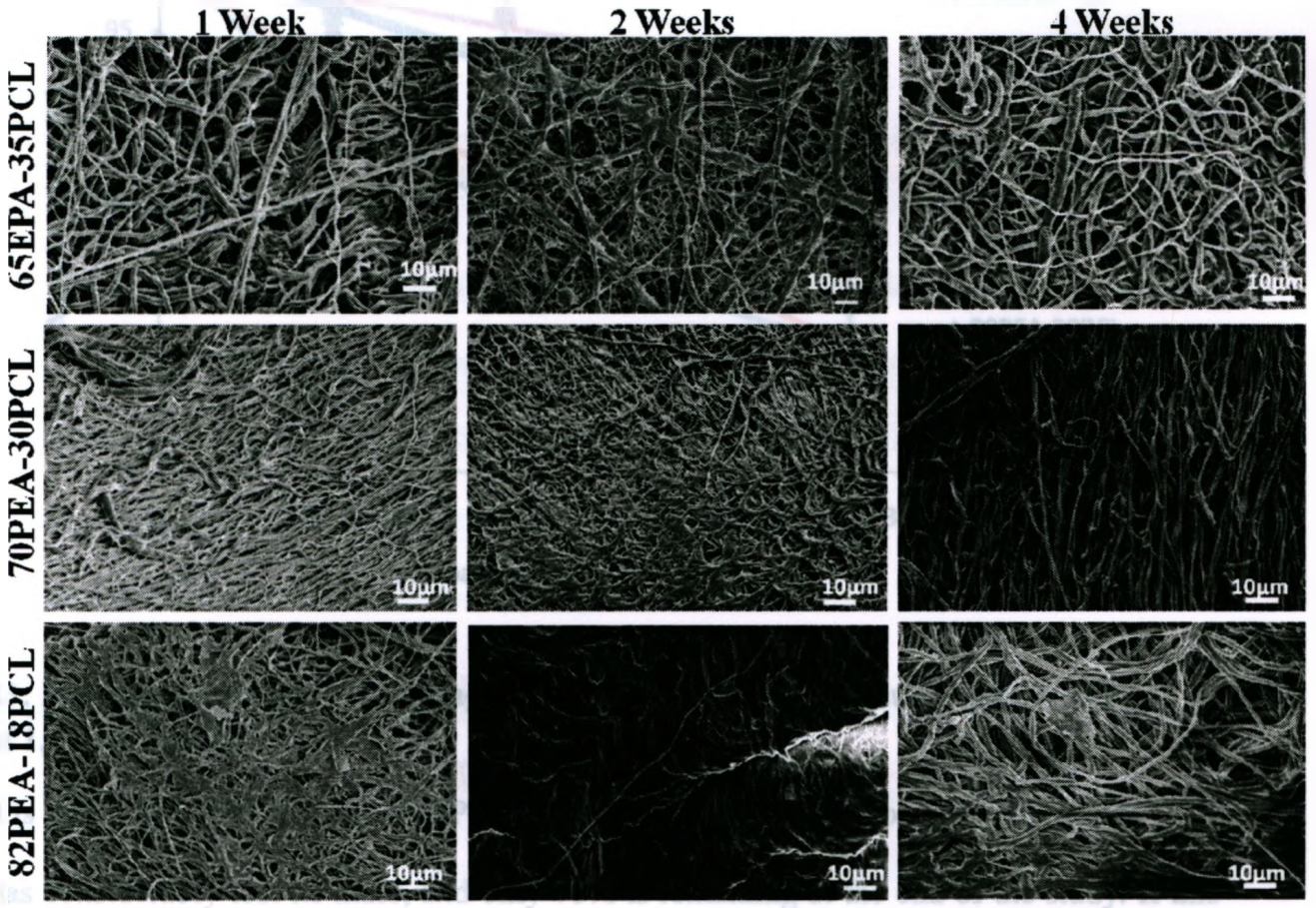

Figure 22: SEM images of electrospun mats at varying concentrations in PBS after 1, 2 and 4 weeks. (A-C) 65PEA-35PCL (D-E) 70PEA-30PCL and (G-I) 82PEA-18PCL

3.3.2 Quantitative Degradation of PEA

Mass loss was used to assess degradation rates in the discs over a time period of 4 weeks. Discs were weighed at the beginning of the experiments and thereafter at each time period, following an overnight drying in a vacuum oven at room temperature. Two separate analyses were computed: (1) the percentage of mass remaining of the discs with respect to degradation time in PBS and (2) the percentage of mass remaining of the discs with respect to PEA composition, over the course of 1, 2 and 4 weeks. It can be deduced from Figure 23 that PEA degrades steadily over time.

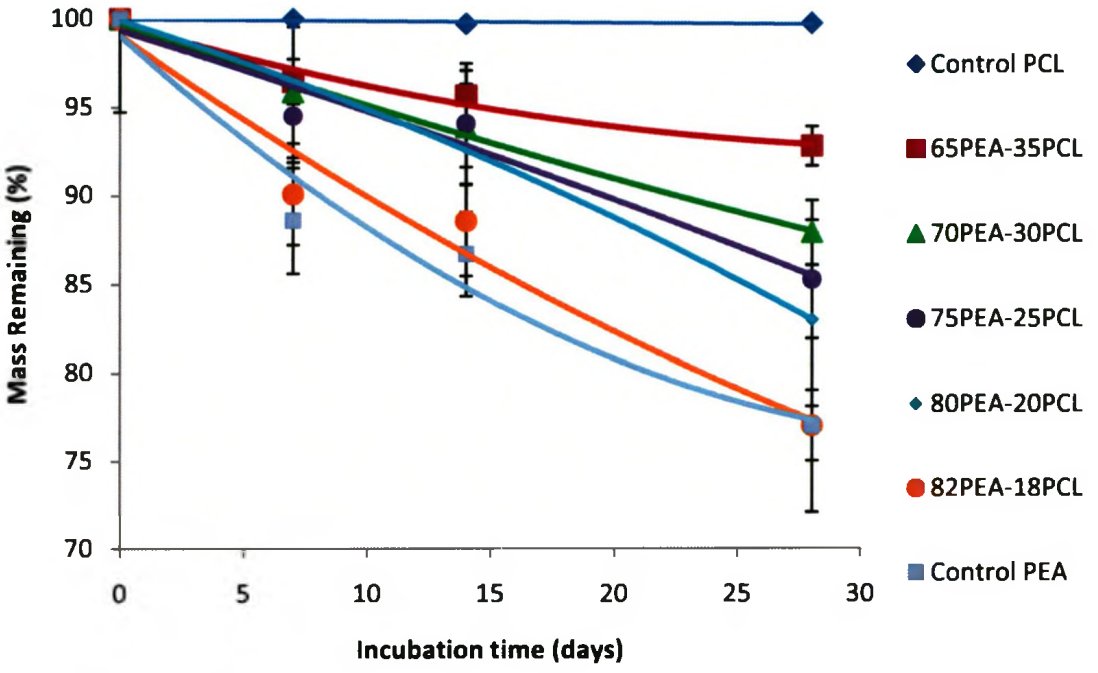

Figure 23: Percentage of mass remaining of all polymer blend discs and controls after a period of 1, 2 and 4 weeks

It is interesting to note that while PCL barely degrades over the span of a month, the PEA control has considerably lost its mass, and only 71% is remaining at the end of the study. If this rate of degradation continues, it will take around 10-12 weeks for complete degradation. Another key trend that can be seen from these curves is that mass loss significantly increased with the increase in quantity of PEA. For example, 65PEA-35PCL shows the least mass loss due to its high percentage of PCL. Although there is not much difference between the degradation rates of the 70PEA-30PCL and 75PEA-25PCL blends, the other concentrations show a steady loss in mass over 4 weeks. Overall, as the amount of PCL was increased, the rate of degradation decreased. This is to be expected given the difference in degradation profiles between the two polymers. It must be noted that although these are discs, the actual scaffolds designed for this study were fabricated by electrospinning. Given the 3-D structure and porous and pliable nature of the electrospun mats, degradation rates would increase significantly for all the polymer

blends. A short time degradation profile such as the one exhibited by PEA is ideal for vascular tissue engineering applications as the construct will degrade since the cells proliferate and migrate around the new tissue.

Analysis of degradation rates with respect to composition also confirmed the above-mentioned results. Figure 24 indicates that over a time period of 4 weeks, the discs with a higher ratio of PEA degraded the fastest, whereas PCL and high PCL ratios (such as 65PEA-35PCL) degraded much slower. At the end of 28 days, this polymer blend had only lost 8.2% of its original mass. This value, when compared to the disc containing PEA-PCL ratios of 82-18, which had degraded 23% of its original mass, is significantly lower.

Quantitative degradation shed new insight on PEA's viability as a tissue engineering scaffold material. A prime candidate for tissue engineering is its ability to degrade while cells attach and infiltrate the scaffold to form new tissue; the profiles exhibited by PEA and all of the polymer blends show promising results for use in cardiovascular constructs.

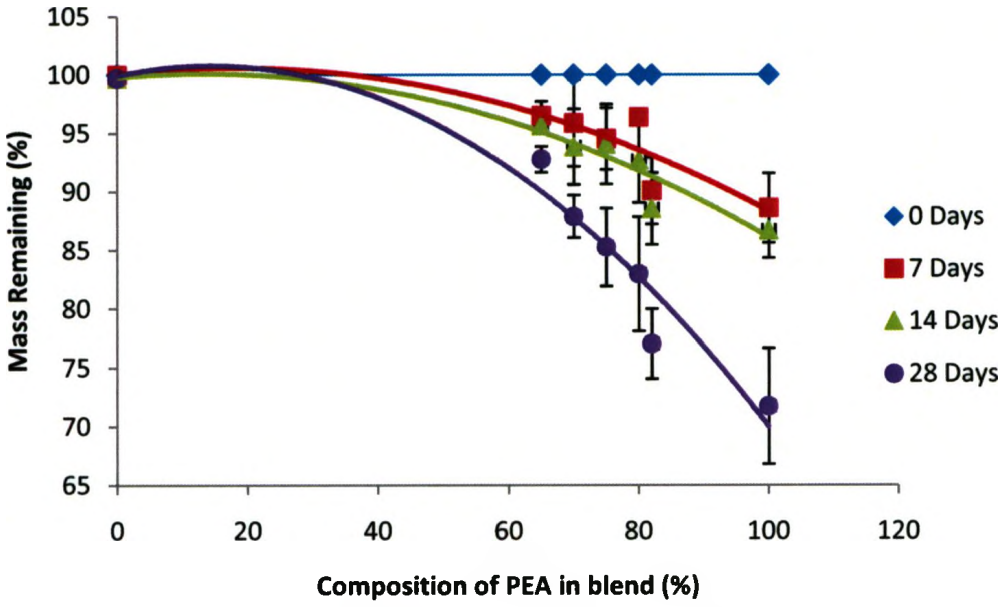

Figure 24: Percentage of mass remaining with respect to PEA concentration of polymer blend discs and controls, at time periods 1, 2 and 4 weeks.

Finally, in order to gain understanding on the mechanism of degradation, GPC was utilized to measure molecular weights of degraded and undegraded polymer. 82PEA-18PCL was chosen as it degraded the fastest of all the polymer blend discs and therefore would be most indicative of molecular weight loss, if any. Figure 25 presents GPC overlays for different time points over the course of 2 weeks to assess mechanism of degradation. As it can be seen, molecular weights stay more or less the same through the 14 days, indicating surface erosion type degradation mechanisms. Molecular weights were measured after 2 hours of incubation in PBS as well; this was carried out in order to eliminate instantaneous leaching that are sometimes prevalent in biodegradable polymers.

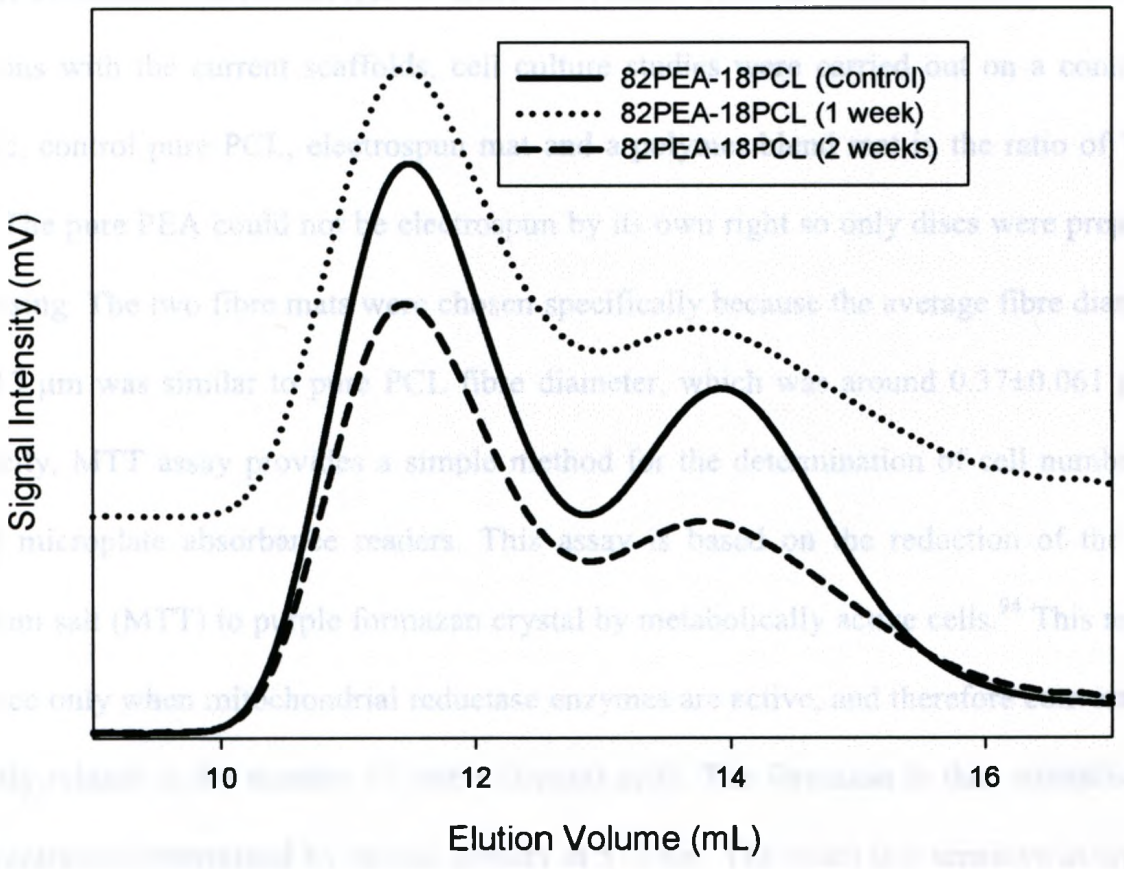

Figure 25: GPC data of 82PEA-18PCL discs at different points during degradation, namely after 1 and 2 weeks.

All the data obtained in the degradation study showed a steady degradation profile without loss of overall molecular weight. This indicates a resilient yet biodegradable polymer that could serve well as a potential scaffold material for vascular tissue engineering.

3.4 Vascular Smooth Muscle Cell Culture Studies

The two critical components in tissue engineering are the cells and the scaffold to which cells can attach and grow.[93] Porous scaffolds, which mimic the natural extracellular matrix, are required for 3-D growth of cells to form *in vitro* tissue engineered constructs. This, in turn, requires that scaffolds should be non-cytotoxic and should promote signaling pathways that influence key cell function such as migration, proliferation, and differentiation. In view of these, it would be important to test the current electrospun scaffolds for cytotoxicity and maintenance of the differentiated cell phenotype. In order to evaluate vascular smooth muscle cell (VSMC) interactions with the current scaffolds, cell culture studies were carried out on a control pure PEA disc, control pure PCL, electrospun mat and a polymer blend mat in the ratio of 70PEA-30PCL. The pure PEA could not be electrospun by its own right so only discs were prepared by heat pressing. The two fibre mats were chosen specifically because the average fibre diameter of 0.41±0.13 μm was similar to pure PCL fibre diameter, which was around 0.37±0.061 μm. For cytotoxicity, MTT assay provides a simple method for the determination of cell number using standard microplate absorbance readers. This assay is based on the reduction of the yellow tetrazolium salt (MTT) to purple formazan crystal by metabolically active cells.[94] This reduction takes place only when mitochondrial reductase enzymes are active, and therefore conversion can be directly related to the number of viable (living) cells. The formazan is then solubilised, and the concentration determined by optical density at 570 nm. The result is a sensitive assay with a colorimetric signal proportional to the cell number.

Figure 26 shows the cytotoxicity data obtained following 4 days and 7 days of culture. At day four, there was no statistical significance between the PEA fibre mat and the pure PCL fibre mat which was used as a control. However, at day seven, cell viability on the 70PEA-30PCL mat was statistically significant suggesting that PEA scaffolds provided a better microenvironment for seeded vascular smooth muscle cells. Between these two samples, there was no difference in the fibre diameter; overruling this to be a factor for the observed cell viability difference. As discussed earlier, pure PCL did not degrade during 7 days incubation whereas 70PEA-30PCL has lost 5% of the initial mass following 7 days of incubation in PBS. Based on this, pure PCL could have been a better scaffold for cell vitality, but this did not seem to be the case. Although the culture time is short and, long-term culture needs to be done, the results indicate the degradation product was not affecting cell viability.

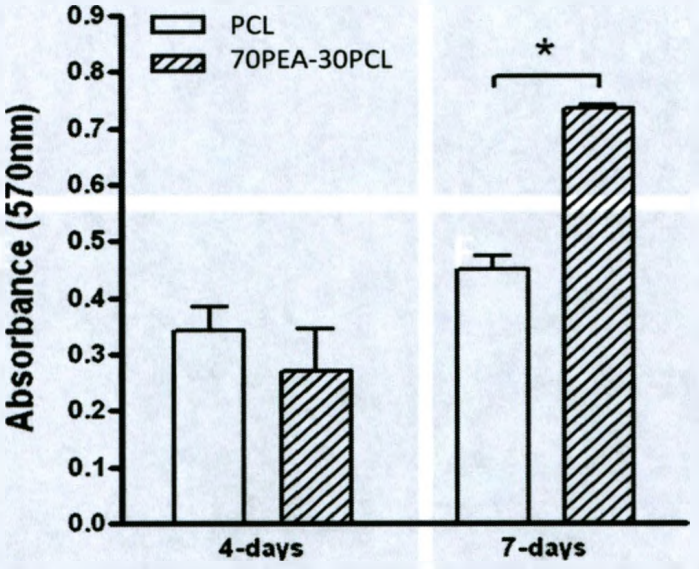

Figure 26: Human coronary artery smooth muscle cell viability on PEA and PCL electrospun fibres. Scaffolds were seeded with a cell density of 6 x 104 cells/scaffold and cultured for 4 and 7 days before MTT treatment. Data are mean±SD for experiments conducted in triplicate. One way ANOVA and post-hoc Tukey comparative tests were used. Solid line coupled with * indicates statistical significance at 95% confidence interval.

Morphologically, HCASMCs were seen well-spread on all surfaces with abundant F-actin as shown in Figure 27. Comparing these images, it appears that cells seeded on the 3-D fibres (both pure PCL and 70PEA-30PCL) were denser than cells seeded on the pure PEA disc.

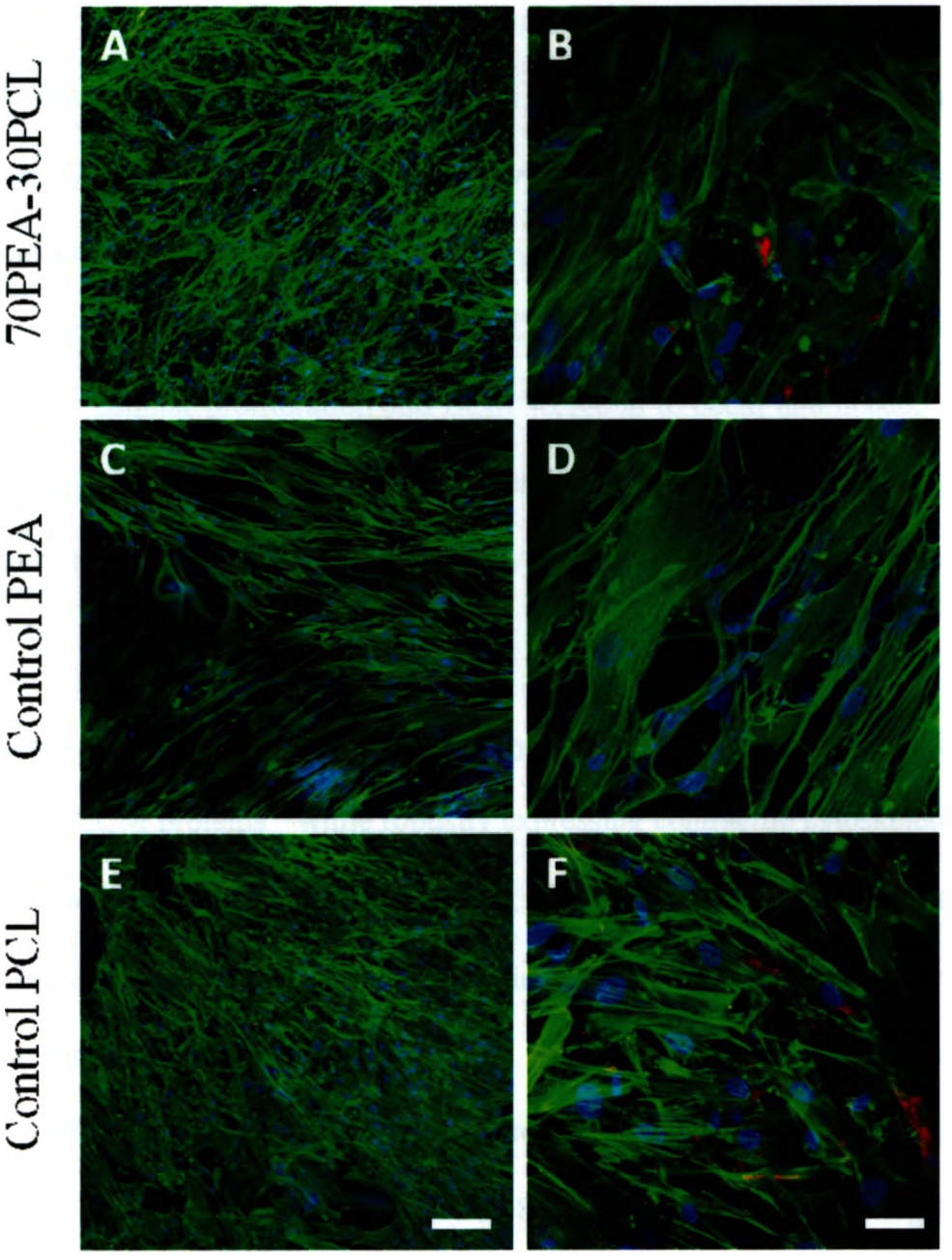

Figure 27: Representative confocal microscopy images of HCASMC cultured on different scaffolds for 4 days. Green represents F-actin (phalloidin stained), blue is for nuclei, and red is for SMC α-actin. Scale bar: 100 μm (A, C, E); 25 μm (B, D, F)

In addition to cell viability, *in vitro* vascular tissue engineering requires that cells be given a more specific level of instruction so that tissue fabrication is successful.[95] However, two interrelated unsolved challenges - regulation of vascular smooth muscle cell phenotype and synthesis of elastin in engineered vascular tissues - significantly hinder progress in this area. Unlike cardiac or skeletal muscle cells, VSMCs are not terminally differentiated and are able to modulate their phenotype in response to changing environmental cues. By understanding and regulating the local environmental cues required for phenotype modulation, living vascular substitutes can be engineered.[96] When cultured on 3D scaffolds, VSMCs must be first in a synthetic phenotype for cellular proliferation and ECM secretion to occur and needed for tissue generation and maturation. The synthetic phenotype is anticipated to accelerate elastin synthesis, a critical extracellular matrix component that is notably absent in currently engineered vascular tissues.

In a contractile phenotype VSMCs have a very low proliferative activity and produce only small amounts of ECM proteins[97] while robustly expressing contractile cytoskeletal marker proteins such as smooth muscle α-actin (SMα-actin); and contract in response to electrical, chemical and mechanical stimuli.[98, 99] Conversely, in a synthetic phenotype they become predominantly proliferative suppress the expression of genes that define the contractile phenotype while rapidly upregulating genes required for proliferation including matrix metalloproteinases and l-caldesmon. Figures 27 and 28 presents the double staining for SMα-actin from which it can be inferred that HCASMC did not express significant levels of the contractile protein indicating a predominantly synthetic phenotype. Although the data is limited to draw a comprehensive conclusion, it suggests that for up to 7 days culture the PEA scaffolds were able to induce a synthetic phenotype.

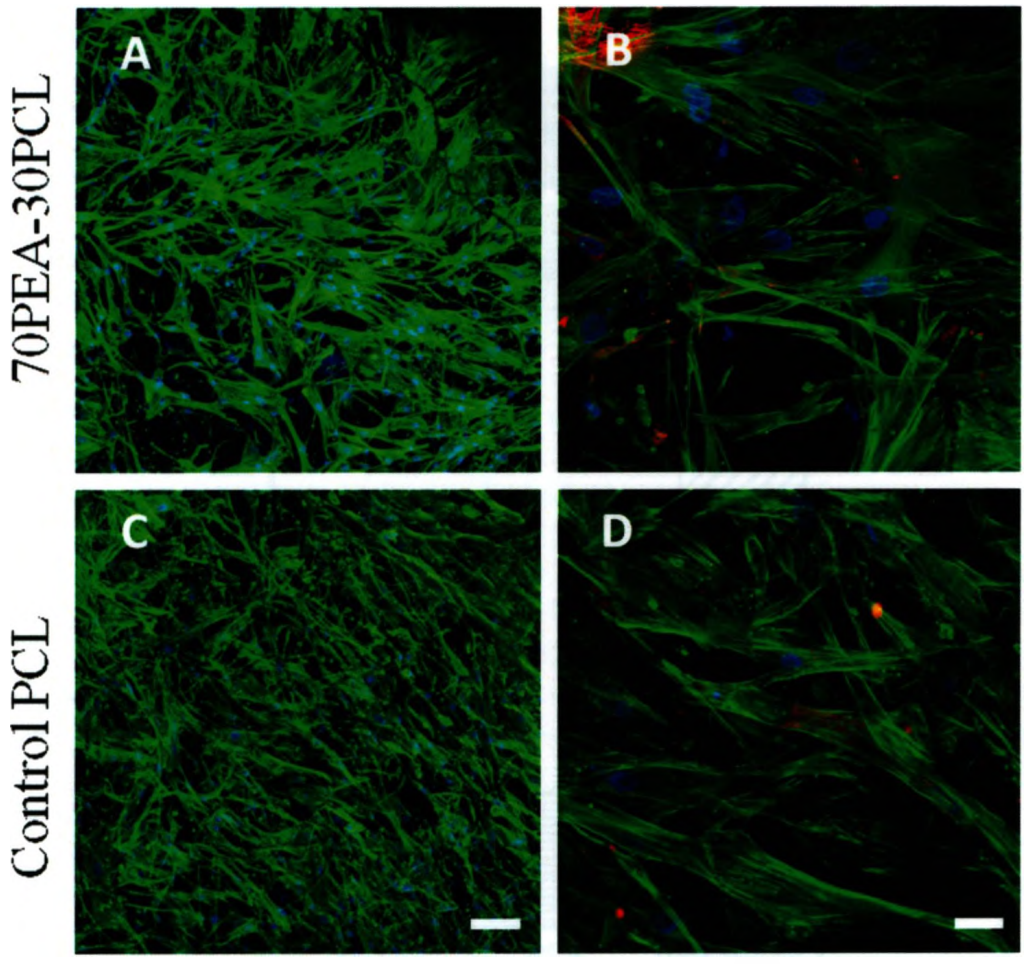

Figure 28: Representative confocal microscopy images of HCASMC cultured on different scaffolds for 7 days. Green represents F-actin (phalloidin stained), blue is for nuclei, and red is for SMC α-actin. Scale bar: 100 μm (A, C); 25 μm (B, D)

To evaluate the possibility that reduced contractile marker protein expression may lead to enhanced elastin gene expression, Western blot analysis was conducted. Figure 29 shows elastin expression data at 7 days culture from which it is clear that 70PEA-30PCL fibrous scaffold expressed a significantly higher elastin protein compared with the Pure PEA and pure PCL controls. This data is consistent with the MTT assay where 70PEA-30PCL had enhanced cell viability.

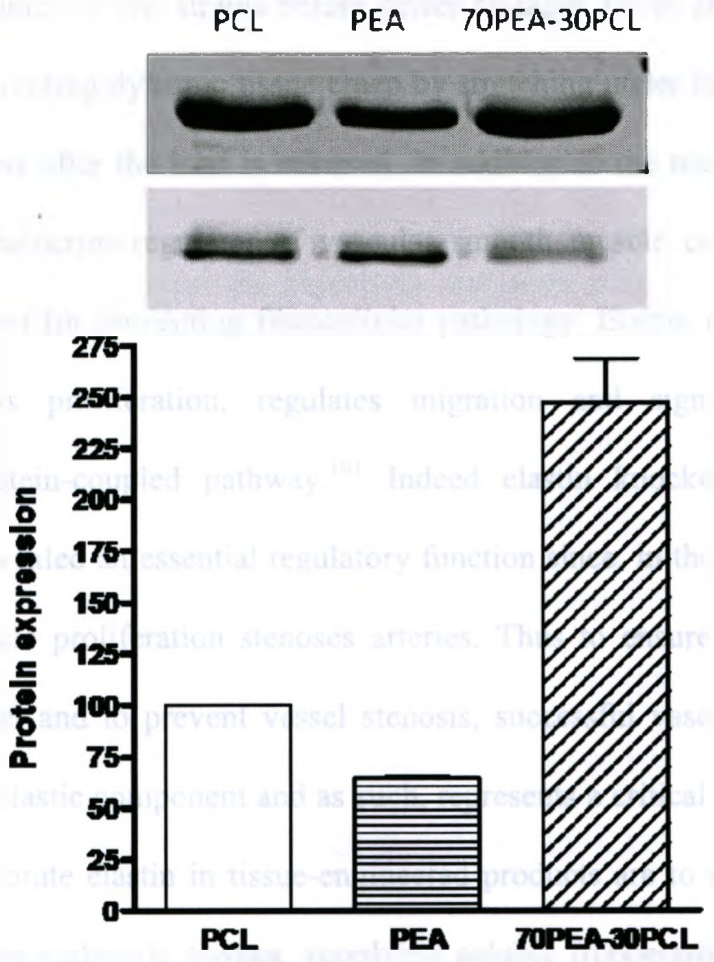

Figure 29: Synthesis of elastin by HCASMCs cultured for 7 days in pure PCL, pure PEA and 70PEA-30PCL fibrous scaffold as determined by western blot analysis. The densities of protein expression were quantified and normalized to the expression levels of GAPDH. Data are all mean ± SEM. Data are mean ±SD for 3 independent experiments.

Taken together, the current study strongly suggest that biodegradable PEA fibrous scaffolds to be a viable candidate for vascular tissue engineering that may regulate cell phenotype and promote elastin synthesis.

An appropriately responsive tissue-engineered blood vessel should possess sufficient mechanical strength, compliance, and suture retention, all of which are governed by the vascular extracellular matrix. The major matrix components of the vascular wall are elastin and Type I collagen produced by VSMCs. While collagen provides the stiffness of the vessel wall, elastin

dictates tissue mechanics at low strains before stiffer collagen fibres are engaged.[100] They also confer elasticity, preventing dynamic tissue creep by stretching under load and recoiling to their original configurations after the load is released. In addition to the mechanical responsiveness, elastin is a potent autocrine regulator of vascular smooth muscle cell activity and that this regulation is important for preventing fibrocellular pathology. Elastin induces actin stress fibre organization, inhibits proliferation, regulates migration and signals via a non-integrin heterotrimeric G-protein-coupled pathway.[101] Indeed elastin knockout studies and clinical observations have revealed an essential regulatory function since, in the absence of extracellular elastin, smooth muscle proliferation stenoses arteries. Thus to ensure appropriate mechanical function of the vessel and to prevent vessel stenosis, successful vascular tissue replacements must incorporate an elastic component and as such, represents a critical design goal. The current approaches to incorporate elastin in tissue-engineered products are to utilize exogenous elastin scaffold isolated from cadaveric tissues, supplying soluble tropoelastin to a cell culture, and designing biocompatible synthetic elastic polymers.[102, 103] Thus fundamental understanding on VSMCs phenotype regulation and as well as scaffold material selection is vitally important. The present study suggests that the phenotype of smooth muscle cells in 3-D engineered vascular tissues is regulated by the chemistry of the scaffold.

CHAPTER 4

4 Conclusions and Future Directions

4.1 Conclusions

In this study, attempts to meet the objectives that were outlined in Chapter 1 have been fulfilled. First, a new polymer with both ester and amino groups consisting of L-alanine, 1,8-octanediol and sebacic acid was synthesized successfully, as confirmed by spectroscopic studies. This polymer, in conjunction with PCL, was used to fabricate 3-D scaffolds by electrospinning. Although a blend with PCL was finally used in order to achieve the scaffolds, it was shown that composition ratio had little effect on fibre diameter. Solution concentration was shown to be one of the most important factors in assessing average fibre size as well as pore size distributions. With increasing polymer concentration, the fibre size increased, in turn increasing the pore size of the electrospun mat. The effect of distance to the collector on fibre size was also studied and, it was shown that increasing the collector distance reduced the average fibre diameter. Degradation studies revealed that the amount of PEA in the polymer blends had a direct effect on the eventual degradation rate. Pure PEA showed a mass loss of 33% at the end of one month incubation in PBS at 37°C. HCASMCs cultured on these materials indicated that the scaffolds were not cytotoxic. In addition, Western blot analysis confirmed the expression of the protein elastin. This study suggested a possible utility of the newly synthesized PEA for vascular tissue engineering applications.

4.2 Future Directions

Given the limited scope and timeline of the project, detailed thermal and physicochemical analyses of the PEA-PCL blends were not conducted. It is suggested that these studies be carried out in order to understand the properties of the PEA-PCL blends.

As most of the cell culture studies were done on short-term basis, it would be useful to expand the scope and carry out long-term investigation. Growing the cells on the scaffolds in a bioreactor would also help assess the viability of the engineered constructs from these scaffolds. Mechanical properties of the scaffolds such as tensile strength should also be studied. Since degradation studies in this work focused only on scaffold integrity in PBS, it is important to conduct an enzymatic study as well. Finally, cell differentiation should also be assessed to further understand the role of PEAs in tissue engineering for vascular constructs.

References

1. Lloyd-Jones D, Adams R, Carnethon M, De Simone G, Ferguson TB, Flegal K, Ford E, Furie K, Go A, Greenlund K et al: Heart disease and stroke statistics--2009 update: a report from the American Heart Association Statistics Committee and Stroke Statistics Subcommittee, Circulation 2009, 119:e21-181

2. Chen HC, Hu YC: Bioreactors for Tissue Engineering, Biotechnology Letters 2006, 28:1415

3. Manuel DG, Leung M, Nguyen K, Tanuseputro P, Johansen H: Burden of cardiovascular disease in Canada, Canadian Journal of Cardiology 2003, 19:997-1004

4. Chen Q-Z, Harding SE, Ali NN, Lyon AR, Boccaccini AR: Biomaterials in cardiac tissue engineering: Ten years of research survey, Materials Science and Engineering: R: Reports 2008, 59:1-37

5. Barron V, Lyons E, Stenson-Cox C, McHugh PE, Pandit A: Bioreactors for Cardiovascular Cell and Tissue Growth: A Review, Annals of Biomedical Engineering 2003, 31:1017-1030

6. Zammaretti P, Jaconi M: Cardiac tissue engineering: regeneration of the wounded heart, Current opinion in biotechnology 2004, 15:430-434

7. L'Heureux N, Dusserre N, Konig G, Victor B, Keire P, Wight TN, Chronos NAF, Kyles AE, Gregory CR, Hoyt G, Robbins RC, McAllister TN: Human tissue-engineered blood vessels for adult arterial revascularization, Nature medicine 2006, 12:361-365

8. Baguneid MS, Seifalian AM, Salacinski HJ, Murray D, Hamilton G, Walker MG: Tissue engineering of blood vessels, British Journal of Surgery 2006, 93:282-290

9. Ertl G, Thum T: New Insight Into Healing Mechanisms of the Infarcted Heart, Journal of the American College of Cardiology 2010, 55:144-146

10. Orlic D, Hill JM, Arai AE: Stem cells for myocardial regeneration, Circ Res 2002, 91:1092-1102

11. Orlic D: Adult BM stem cells regenerate mouse myocardium, Cytotherapy 2002, 4:521-525

12. Haskal ZJ, Trerotola S, Dolmatch B, Schuman E, Altman S, Mietling S, Berman S, McLennan G, Trimmer C, Ross J, Vesely T: Stent graft versus balloon angioplasty for failing dialysis-access grafts, N Engl J Med 2010, 362:494-503

13. Venkatraman S, Boey F: Release profiles in drug-eluting stents: Issues and uncertainties, Journal of Controlled Release 2007, 120:149-160

14. Alexander KP, Anstrom KJ, Muhlbaier LH, Grosswald RD, Smith PK, Jones RH, Peterson ED: Outcomes of cardiac surgery in patients > or = 80 years: results from the National Cardiovascular Network, J Am Coll Cardiol 2000, 35:731-738

15. Rabkin E, Schoen FJ: Cardiovascular tissue engineering, Cardiovascular Pathology 2002, 11:305-317

16. Ratcliffe A: Tissue engineering of vascular grafts, Matrix Biology 2000, 19:353-357

17. Davies MG, Hagen PO: Pathophysiology of vein graft failure: a review, Eur J Vasc Endovasc Surg 1995, 9:7-18

18. Sunderdiek U, Kalweit GA, Marx R, Schipke JD, Gams E: Minimally invasive coronary artery bypass grafting in high-risk patients. Late follow-up with assessment of left internal mammary artery graft patency and flow by exercise transthoracic Doppler echocardiography, Cardiovasc Surg 2003, 11:389-395

19. Akhyari P, Kamiya H, Haverich A, Karck M, Lichtenberg A: Myocardial tissue engineering: the extracellular matrix, European Journal of Cardio-Thoracic Surgery 2008, 34:229-241

20. Lee J, Cuddihy MJ, Kotov NA: Three-dimensional cell culture matrices: state of the art, Tissue Engineering Part B: Reviews 2008, 14:61-86

21. Agarwal S, Wendorff JH, Greiner A: Progress in the Field of Electrospinning for Tissue Engineering Applications, Advanced Materials 2009, 21:3343-3351

22. Howard D, Buttery LD, Shakesheff KM, Roberts SJ: Tissue engineering: strategies, stem cells and scaffolds, Journal of anatomy 2008, 213:66-72

23. Vesely I: Heart valve tissue engineering, Circulation research 2005, 97:743-755

24. Gong Z, Niklason LE: Blood vessels engineered from human cells, Trends in cardiovascular medicine 2006, 16:153-156

25. Stephan S, Ball SG, Williamson M, Bax DV, Lomas A, Shuttleworth CA, Kielty CM: Cell-matrix biology in vascular tissue engineering, Journal of anatomy 2006, 209:495-502

26. Martin Y, Vermette P: Bioreactors for tissue mass culture: Design, characterization, and recent advances, Biomaterials 2005, 26:7481-7503

27. Lutolf MP, Hubbell JA: Synthetic biomaterials as instructive extracellular microenvironments for morphogenesis in tissue engineering, Nat Biotechnol 2005, 23:47-55

28. Hoerstrup SP, Zünd G, Sodian R, Schnell AM, Grünenfelder J, Turina MI: Tissue engineering of small caliber vascular grafts, European Journal of Cardio-thoracic Surgery 2001, 20:164-169

29. L'Heureux N, Dusserre N, Konig G, Victor B, Keire P, Wight TN, Chronos NA, Kyles AE, Gregory CR, Hoyt G, Robbins RC, McAllister TN: Human tissue-engineered blood vessels for adult arterial revascularization, Nat Med 2006, 12:361-365

30. Chlupac J, Filova E, Bacakova L: Blood vessel replacement: 50 years of development and tissue engineering paradigms in vascular surgery, Physiol Res 2009, 58 Suppl 2:S119-139

31. McAllister TN, Maruszewski M, Garrido SA, Wystrychowski W, Dusserre N, Marini A, Zagalski K, Fiorillo A, Avila H, Manglano X, Antonelli J, Kocher A, Zembala M, Cierpka L, de la Fuente LM, L'Heureux N: Effectiveness of haemodialysis access with an autologous tissue-engineered vascular graft: a multicentre cohort study, Lancet 2009, 373:1440-1446

32. Petersen MC, Lazar J, Jacob HJ, Wakatsuki T: Tissue engineering: a new frontier in physiological genomics, Physiol Genomics 2007, 32:28-32

33. Kim JB: Three-dimensional tissue culture models in cancer biology, Semin Cancer Biol 2005, 15:365-377

34. Schanz J, Pusch J, Hansmann J, Walles H: Vascularised human tissue models: a new approach for the refinement of biomedical research, J Biotechnol 2010, 148:56-63

35. Hansen A, Eder A, Bonstrup M, Flato M, Mewe M, Schaaf S, Aksehirlioglu B, Schworer A, Uebeler J, Eschenhagen T: Development of a drug screening platform based on engineered heart tissue, Circ Res 2010, 107:35-44

36. L'Heureux N, Stoclet JC, Auger FA, Lagaud GJ, Germain L, Andriantsitohaina R: A human tissue-engineered vascular media: a new model for pharmacological studies of contractile responses, FASEB J 2001, 15:515-524

37. Katare RG, Ando M, Kakinuma Y, Sato T: Engineered heart tissue: a novel tool to study the ischemic changes of the heart in vitro, PLoS One 2010, 5:e9275

38. Huh D, Matthews BD, Mammoto A, Montoya-Zavala M, Hsin HY, Ingber DE: Reconstituting organ-level lung functions on a chip, Science 2010, 328:1662-1668

39. Reichl S, Dohring S, Bednarz J, Muller-Goymann CC: Human cornea construct HCC-an alternative for in vitro permeation studies? A comparison with human donor corneas, Eur J Pharm Biopharm 2005, 60:305-308

40. Verbridge SS, Choi NW, Zheng Y, Brooks DJ, Stroock AD, Fischbach C: Oxygen-controlled three-dimensional cultures to analyze tumor angiogenesis, Tissue Eng Part A 2010, 16:2133-2141

41. Raimondi MT: Engineered tissue as a model to study cell and tissue function from a biophysical perspective, Curr Drug Discov Technol 2006, 3:245-268

42. Brooke BS, Bayes-Genis A, Li DY: New insights into elastin and vascular disease, Trends in cardiovascular medicine 2003, 13:176-181

43. Buijtenhuijs P, Buttafoco L, Poot AA, Daamen WF, van Kuppevelt TH, Dijkstra PJ, de Vos RAI, Sterk LMT, Geelkerken BRH, Feijen J, Vermes I: Tissue engineering of blood vessels: Characterization of smooth-muscle cells for culturing on collagen-and-elastin-based scaffolds, Biotechnology and applied biochemistry 2004, 39:141-149

44. Vepari C, Kaplan DL: Silk as a biomaterial, Progress in Polymer Science 2007, 32:991-1007

45. Beachley V, Wen X: Polymer nanofibrous structures: Fabrication, biofunctionalization, and cell interactions, Progress in Polymer Science 2010, 35:868-892

46. Barnes CP, Sell SA, Boland ED, Simpson DG, Bowlin GL: Nanofiber technology: Designing the next generation of tissue engineering scaffolds, Advanced Drug Delivery Reviews 2007, 59:1413-1433

47. Feugier P, Black RA, Hunt JA, How TV: Attachment, morphology and adherence of human endothelial cells to vascular prosthesis materials under the action of shear stress, Biomaterials 2005, 26:1457-1466

48. Ma H, Hu J, Ma PX: Polymer Scaffolds for Small-Diameter Vascular Tissue Engineering, Advanced Functional Materials 2010, 20:2833-2841

49. Bramfeldt H, Sarazin P, Vermette P: Smooth muscle cell adhesion in surface-modified three-dimensional copolymer scaffolds prepared from co-continuous blends, Journal of Biomedical Materials Research Part A 2008, 2008/11/05

50. Isenberg BC, Williams C, Tranquillo RT: Small-diameter artificial arteries engineered in vitro, Circulation research 2006, 98:25-35

51. Lee KY, Jeong L, Kang YO, Lee SJ, Park WH: Electrospinning of polysaccharides for regenerative medicine, Advanced Drug Delivery Reviews 2009, 61:1020-1032

52. Dahl SL, Koh J, Prabhakar V, Niklason LE: Decellularized native and engineered arterial scaffolds for transplantation, Cell transplantation 2003, 12:659-666

53. Amiel GE, Komura M, Shapira O, Yoo JJ, Yazdani S, Berry J, Kaushal S, Bischoff J, Atala A, Soker S: Engineering of blood vessels from acellular collagen matrices coated with human endothelial cells, Tissue engineering 2006, 12:2355-2365

54. Nisbet DR, Forsythe JS, Shen W, Finkelstein DI, Horne MK: Review Paper: A Review of the Cellular Response on Electrospun Nanofibers for Tissue Engineering, Journal of Biomaterials Applications 2009, 24:7-29

55. Sakiyama-Elbert SE, Hubbell JA: Functional Biomaterials: Design of Novel Biomaterials, Annual Review of Materials Research 2001, 31:183-201

56. Day RM, Maquet V, Boccaccini AR, Jérôme R, Forbes A: In vitro and in vivo analysis of macroporous biodegradable poly(D,L-lactide-co-glycolide) scaffolds containing bioactive glass, Journal of Biomedical Materials Research Part A 2005, 75A:778-787

57. Puiggali J, Ikada Y, Tsuji H, Cartier L, Okihara T, Lotz B: The frustrated structure of poly(-lactide), Polymer 2000, 41:8921-8930

58. Liu KL, Choo ES, Wong SY, Li X, He CB, Wang J, Li J: Designing poly[(R)-3-hydroxybutyrate]-based polyurethane block copolymers for electrospun nanofiber scaffolds with improved mechanical properties and enhanced mineralization capability, J Phys Chem B 2010, 114:7489-7498

59. Anderson JM: Biological responses to materials, Annual Review of Materials Science 2001, 31:81-110

60. Gunatillake P, Mayadunne R, Adhikari R: Recent developments in biodegradable synthetic polymers, Biotechnology annual review 2006, 12:301-347

61. Heydarkhan-Hagvall S, Esguerra M, Helenius G, Soderberg R, Johansson BR, Risberg B: Production of extracellular matrix components in tissue-engineered blood vessels, Tissue engineering 2006, 12:831-842

62. Vesely I: The evolution of bioprosthetic heart valve design and its impact on durability, Cardiovascular Pathology 2003, 12:277-286

63. Greenwald SE, Berry CL: Improving vascular grafts: The importance of mechanical and haemodynamic properties, Journal of Pathologoy 2000, 190:292-299

64. Grenier S, Sandig M, Mequanint K: Polyurethane biomaterials for fabricating 3D porous scaffolds and supporting vascular cells, Journal of Biomedical Materials Research Part A 2007, 82A:802

65. Grenier S, Sandig M, Holdsworth DW, Mequanint K: Interactions of coronary artery smooth muscle cells with 3D porous polyurethane scaffolds, Journal of Biomedical Materials Research Part A 2008,

66. Martina M, Hutmacher DW: Biodegradable polymers applied in tissue engineering research: a review, Polymer International 2007, 56:145-157

67. Puiggalí J, Subirana JA: Synthetic polymers containing α-amino acids: From polyamides to poly(ester amide)s, Journal of Peptide Science 2005, 11:247-249

68. Horwitz JA, Shum KM, Bodle JC, Deng M, Chu CC, Reinhart-King CA: Biological performance of biodegradable amino acid-based poly(ester amide)s: Endothelial cell adhesion and inflammation in vitro, J Biomed Mater Res A 2010, 95:371-380

69. Paredes N, Rodriguez-Galán A, Puiggalí J, Peraire C: Studies on the biodegradation and biocompatibility of a new poly(ester amide) derived from L-alanine, Journal of Applied Polymer Science 1998, 69:1537-1549

70. Paredes N, Rodríguez-Galán A, Puiggalí J: Synthesis and characterization of a family of biodegradable poly(ester amide)s derived from glycine, Journal of Polymer Science, Part A: Polymer Chemistry 1998, 36:1271-1282

71. Rodríguez-Galán A, Fuentes L, Puiggalí J: Studies on the degradability of a poly(ester amide) derived from L-alanine, 1,12-dodecanediol and 1,12-dodecanedioic acid, Polymer 2000, 41:5967-5970

72. Rodríguez-Galán A, Pelfort M, Aceituno JE, Puiggalí J: Comparative studies on the degradability of poly(ester amide)s derived from L- and L,D-alanine, Journal of Applied Polymer Science 1999, 74:2312-2320

73. Guo K, Chu CC: Controlled release of paclitaxel from biodegradable unsaturated poly(ester amide)s/poly(ethylene glycol) diacrylate hydrogels, Journal of Biomaterials Science-Polymer Edition 2007, 18:489-504

74. Katsarava R, Beridze V, Arabuli N, Kharadze D, Chu CC, Won CY: Amino Acid-Based Bioanalogous Polymers. Synthesis, and Study of Regular Poly(ester amide)s Based on Bis(a-amino acid) α,ω-Alkylene Diesters, and Aliphatic Dicarboxylic Acids, Journal of Polymer Science, Part A: Polymer Chemistry 1999, 37:391-407

75. Guo K, Chu CC: Biodegradable and injectable paclitaxel-loaded poly(ester amide)s microspheres: Fabrication and characterization, Journal of Biomedical Materials Research - Part B Applied Biomaterials 2009, 89:491-500

76. Whang K, Thomas CH, Healy KE, Nuber G: A novel method to fabricate bioabsorbable scaffolds, Polymer 1995, 36:837-842

77. Lee SJ, Liu J, Oh SH, Soker S, Atala A, Yoo JJ: Development of a composite vascular scaffolding system that withstands physiological vascular conditions, Biomaterials 2008, 29:2891-2898

78. Moroni L, De Wijn JR, Van Blitterswijk CA: Integrating novel technologies to fabricate smart scaffolds, Journal of Biomaterials SciencePolymer Edition 2008, 19:543-572

79. Sill TJ, von Recum HA: Electrospinning: Applications in drug delivery and tissue engineering, Biomaterials 2008, 29:1989-2006

80. Xie J, Li X, Xia Y: Putting Electrospun Nanofibers to Work for Biomedical Research, Macromolecular Rapid Communications 2008, 29:1775-1792

81. Pham QP, Sharma U, Mikos AG: Electrospinning of Polymeric Nanofibers for Tissue Engineering Applications: A Review, Tissue engineering 2006, 12:1197

82. Courtney T, Sacks MS, Stankus J, Guan J, Wagner WR: Design and analysis of tissue engineering scaffolds that mimic soft tissue mechanical anisotropy, Biomaterials 2006, 27:3631-3638

83. Shin H, Jo S, Mikos AG: Biomimetic materials for tissue engineering, Biomaterials 2003, 24:4353-4364

84. Katsarava R, Beridze V, Arabuli N, Kharadze D, Chu CC, Won CY: Amino acid-based bioanalogous polymers. Synthesis, and study of regular poly(ester amide)s based on bis(α-amino acid) α,ω-alkylene diesters, and aliphatic dicarboxylic acids, Journal of Polymer Science Part A: Polymer Chemistry 1999, 37:391-407

85. Nava D, Salom C, Prolongo MG, Masegosa RM: Thermal properties and interactions in blends of poly(ε-caprolactone) with unsaturated polyester resins, Proceedings of the International Conference on the Advanced Materials Processing Technology, 2001 2003, 143-144:171-174

86. Thomas V, Jose MV, Chowdhury S, Sullivan JF, Dean DR, Vohra YK: Mechano-morphological studies of aligned nanofibrous scaffolds of polycaprolactone fabricated by electrospinning, Journal of Biomaterials Science -- Polymer Edition 2006, 17:969-984

87. Li L, Chu CC: Nitroxyl radical incorporated electrospun biodegradable poly(ester amide) nanofiber membranes, Journal of Biomaterials Science 2009, 20:341-361

88. Williamson MR, Black R, Kielty C: PCL-PU composite vascular scaffold production for vascular tissue engineering: Attachment, proliferation and bioactivity of human vascular endothelial cells, Biomaterials 2006, 27:3608-3616

89. Son WK, Youk JH, Lee TS, Park WH: The effects of solution properties and polyelectrolyte on electrospinning of ultrafine poly(ethylene oxide) fibers, Polymer 2004, 45:2959-2966

90. Chen M, Zamora PO, Som P, Peña LA, Osaki S: Cell attachment and biocompatibility of polytetrafluoroethylene (PTFE) treated with glow-discharge plasma of mixed ammonia and oxygen, Journal of Biomaterials Science - Polymer Edition 2003, 14:917

91. Murugan R, Ramakrishna S: Design strategies of tissue engineering scaffolds with controlled fiber orientation, Tissue Eng 2007, 13:1845-1866

92. Labet M, Thielemans W: Synthesis of polycaprolactone: a review, Chem Soc Rev 2009, 38:3484-3504

93. Griffith LG: Emerging design principles in biomaterials and scaffolds for tissue engineering, Ann N Y Acad Sci 2002, 961:83-95

94. Cory AH, Owen TC, Barltrop JA, Cory JG: Use of an aqueous soluble tetrazolium/formazan assay for cell growth assays in culture, Cancer Commun 1991, 3:207-212

95. Bottaro DP, Liebmann-Vinson A, Heidaran MA: Molecular signaling in bioengineered tissue microenvironments, Ann N Y Acad Sci 2002, 961:143-153

96. Chan-Park MB, Shen JY, Cao Y, Xiong Y, Liu Y, Rayatpisheh S, Kang GC, Greisler HP: Biomimetic control of vascular smooth muscle cell morphology and phenotype for functional tissue-engineered small-diameter blood vessels, J Biomed Mater Res A 2009, 88:1104-1121

97. Wamhoff BR, Bowles DK, Owens GK: Excitation-transcription coupling in arterial smooth muscle, Circ Res 2006, 98:868-878

98. Owens GK: Regulation of differentiation of vascular smooth muscle cells, Physiol Rev 1995, 75:487-517

99. Rensen SS, Thijssen VL, De Vries CJ, Doevendans PA, Detera-Wadleigh SD, Van Eys GJ: Expression of the smoothelin gene is mediated by alternative promoters, Cardiovasc Res 2002, 55:850-863

100. Bank AJ, Wang H, Holte JE, Mullen K, Shammas R, Kubo SH: Contribution of collagen, elastin, and smooth muscle to in vivo human brachial artery wall stress and elastic modulus, Circulation 1996, 94:3263-3270

101. Karnik SK, Brooke BS, Bayes-Genis A, Sorensen L, Wythe JD, Schwartz RS, Keating MT, Li DY: A critical role for elastin signaling in vascular morphogenesis and disease, Development 2003, 130:411-423

102. Stone PJ, Morris SM, Griffin S, Mithieux S, Weiss AS: Building Elastin. Incorporation of recombinant human tropoelastin into extracellular matrices using nonelastogenic rat-1 fibroblasts as a source for lysyl oxidase, Am J Respir Cell Mol Biol 2001, 24:733-739

103. Berglund JD, Nerem RM, Sambanis A: Incorporation of intact elastin scaffolds in tissue-engineered collagen-based vascular grafts, Tissue Eng 2004, 10:1526-1535

Appendix A: Derivative decomposition temperatures of Polymer blends and Controls